Skull Anatomy of the Miniaturized Gecko *Sphaerodactylus roosevelti* (Squamata: Gekkota)

Juan D. Daza,[1]* Virginia Abdala,[2] Richard Thomas,[1] and Aaron M. Bauer[3]

[1]*Biology Department, University of Puerto Rico, San Juan, Puerto Rico 003931-3360*
[2]*CONICET, Facultad de Ciencias Naturales, Universidad Nacional de Tucumán e Instituto de Herpetología, Fundación Miguel Lillo, Miguel Lillo 251, 4000 Tucumán, Argentina*
[3]*Biology Department, Villanova University, 800 Lancaster Avenue, Villanova, Pennsylvania 19085-1699*

ABSTRACT A detailed description of the skull and jaw of the gecko *Sphaerodactylus roosevelti* is presented. The bones are described articulated and isolated with special consideration given to the type of suture among joining elements. *S. roosevelti* was compared with 109 gekkotan species to evaluate the osteological variation and to find characters for cladistic analysis. Changes in the skull associated with the miniaturization process are discussed within the sphaerodactylid geckos. A noticeable increase of overlapping sutures was observed in the snout of the smallest sphaerodactylids compared to other gekkotans. This pattern is convergent with that in miniaturized pygopodids and may be attributed to adaptations for decreasing mechanical resistance of the cranium during feeding or burrowing. New cranial characters support Sphaerodactylinae as a monophyletic group and should be useful for resolving questions such as their relationship with other gekkotans. J. Morphol. 000:000–000, 2008.

KEY WORDS: Gekkonomorpha; Gekkota; Sphaerodactylidae; Sphaerodactylinae; *Sphaerodactylus roosevelti;* comparative anatomy

The relationships of sphaerodactyl geckos have long been a source of contention. We use the term "sphaerodactyl" to refer to the species of the genera *Coleodactylus, Gonatodes, Lepidoblepharis, Pseudogonatodes,* and *Sphaerodactylus*; sphaerodactylid refers to the entire family, which now includes an array of Old and New World species from miniaturized to large (Gamble et al., 2008a; Fig. 1). Some workers have seen sphaerodactyls as ancient and basal to gekkotans (Underwood, 1954), others as basal within the gekkonids (Han et al., 2004), and yet others have seen them as derived within the gekkonids (Kluge, 1967, 1987, 1995). A factor that may contribute to this uncertainty is the relative lack of detailed anatomical knowledge of the group, perhaps abetted by the difficulty of working with some of the world's smallest lizards (Thomas, 1965; MacLean, 1985; Hedges and Thomas, 2001). Additionally it has been suggested that the head of the sphaerodactyls exhibits many homoplastic characters, mostly because of miniaturization and large eye size (Gamble et al., 2008a). Few if any *Sphaerodactylus* species exceed 40 mm in snout-vent length (Schwartz and Henderson, 1991). For all these reasons we feel that a detailed examination of the cranial skeleton of one species, *Sphaerodactylus roosevelti,* and a comparison with closely related forms, could contribute to a more comprehensive understanding of the group.

The genus *Sphaerodactylus* is the most speciose among gekkotans (93 spp. fide Kluge, 2001). This genus has a mostly circum-Caribbean distribution (King, 1962; Hass, 1991; Hedges and Garrido, 1993; Kluge, 1995; Thomas et al., 1998). *S. roosevelti* is a relatively blunt-headed *Sphaerodactylus*, described once as almost salamander-like (Grant, 1931). It is the largest species in Puerto Rico with a maximum snout-vent length of 39 mm in males (Grant, 1931; Thomas and Schwartz, 1966). We chose this species for a detailed description of skull anatomy based on two criteria, its size and restricted distribution range, which is at the southwest coastal area of the island. We expect that the specimens sampled will cover the variation within the species.

Compared to other squamates, little attention has been focused on the gecko skull (Bauer, 1990a); however, 32 partial and complete descriptions of gekkotan skulls do count 66 extant and three fossil species of gekkotans. A complete list of these descriptions divided into the six recognized gekkotan families (Han et al., 2004; Gamble et al., 2008a) is presented in the Appendix.

Gonatodes is the only genus that has been studied in detail among the sphaerodactylids (Well-

Contract grant sponsors: Graduate Biology Program, Department of Biology, Decanato de Estudios Graduados e Investigación (DEGI) at the University of Puerto Rico-Rio Piedras Campus, NSF; Contract grant number: DEB-0515909.

*Correspondence to: Juan D. Daza, Biology Department, University of Puerto Rico, San Juan, Puerto Rico 003931-3360.
E-mail: juand.daza@gmail.com

Published online in
Wiley InterScience (www.interscience.wiley.com)
DOI: 10.1002/jmor.10664

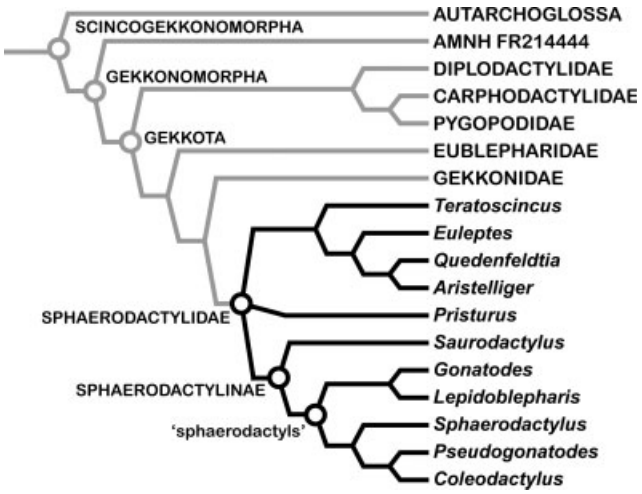

Fig. 1. Relationships of gekkonomorphs, basal relationships follows Conrad and Norell (2006), interfamilial relationships follows Han et al. (2004). Hypothesis within the Sphaerodactylidae follows Gamble et al. (2008a).

born, 1933; Rivero-Blanco, 1976, 1979). *Sphaerodactylus* cranial features have been mentioned concisely in a few works (Noble, 1921; Rieppel, 1984b; Grismer, 1988).

As perhaps the most speciose and successful of all miniaturized lizard lineages, *Sphaerodactylus* provides an ideal starting point for the generation of baseline data for miniaturized lizards. Further, the extensive literature on the skulls of a diversity of other gekkotans, coupled with a robust phylogeny (Han et al., 2004; Gamble et al., 2008a) facilitate an informed comparative approach to the process of miniaturization within this lineage.

This work has two major aims. The first is to present a detailed anatomical description of the head skeleton of *S. roosevelti* discussing some osteological characters. The second is to determine if there are additional skull characteristics attributable to the miniaturization process beyond those that have been identified in more general studies (Rieppel, 1984b, 1996), such as the allometric reduction of the neurocranium relative to the dermatocranium.

MATERIALS AND METHODS

In the description of the characters we emphasize being explicit in order to provide criteria that minimize subjectivity (Poe and Wiens, 2000). We wish to present an updated anatomical nomenclature that can be used in future studies; this is an important step in identifying natural units that can be identified in organisms of different species (Wagner, 2001).

The characters described here reflect primary homology (de Pinna, 1991). We agree that homology is entirely cladogram-dependent and that under this criterion there should not be distinction among primary and secondary (Wheeler, 2005); however, since many characters used to derive gekkotan relationships have not been tested in a broad context, we found it necessary to keep this distinction. Ultimately characters identified here will be usefully interpreted in the context of previous morphological studies (Kluge, 1976; Grismer, 1988; Bauer, 1990a; Kluge, 1995; Abdala, 1998; Conrad and Norell, 2006) and molecular (Donnellan et al., 1999; Ota et al., 1999; Han et al., 2004) approaches.

Specimens were prepared with two different methods. For the analysis of the cranium and jaw with all elements articulated, we cleared and stained with commonly used protocols (Wassersug, 1976; Dingerkus and Uhler, 1977) eight specimens of *S. roosevelti* and 75 specimens of 12 species for comparative purposes. These specimens represent different postnatal ontogenetic stages. Additional articulated material consists of 109 gekkotan species represented by published illustrations and descriptions, digital photographs of dry skulls, and seven CT scanned images from the digital morphology library at the University of Texas (http://digimorph.org/): the Cretaceous gekkonomorph (AMNH FR 21444), *Eublepharis macularius* (CM 67524), *Coleonyx variegatus* (YPM 14383), *Hemitheconyx caudicinctus* (YPM 14381), *Nephrurus levis* (YPM 12868), *Phelsuma lineata* (FMNH 260100), and *Saltuarius cornutus* (FMNH 57503). We use this additional material from published and outside sources for comparative purposes. We center our detailed discussion in the sphaerodactylids for which we have prepared and examined material.

For the analysis of disarticulated bones, we made dry preparations of three specimens (UPRRP 6487, 6489, 6490) by maceration and careful application of sodium hypochlorite (5.25%). The process was monitored with a dissecting microscope to prevent element loss. The action of sodium hypochlorite is fast and can be easily neutralized by immersing the specimen in water. Once tissues are softened, they can be detached with fine-pointed (No. 5) forceps.

Since the works published on gekkotans differ in anatomical terminology and often used different names for bones, foramina, fenestrations, and sutures, most of the terms follow terminology used in recent publications (Bell et al., 2003; Torres-Carvajal, 2003; Conrad, 2004; Evans et al., 2004; Montero et al., 2004; Bever et al., 2005; Evans and Klembara, 2005; Conrad and Norell, 2006).

For the illustrations, specimen UPRRP 6381 was photographed with an 8.0 MP Sony DSC-F828 digital still camera, mounted on a Leica MS5 dissecting microscope. Photos were taken at different magnifications and orientations (34 dorsal, 51 lateral, 38 ventral, and 52 jaw). The illustrations were drawn directly on the pictures with the aid of Adobe® Illustrator® CS3 13.0.2; this method is more precise than traditional Camera Lucida drawings because structures can be traced at higher magnification and combined later; it also allows multiple corrections, providing a more precise outline of the specimen. Measurements from this specimen were obtained from the digital pictures with tpsDig2 v2.05 (Rohlf, 2006). Each measurement was made three times and the mean was calculated. The cleared and stained specimen illustrated (see Fig. 2) is an adult female of *S. roosevelti* from the Bosque Estatal de Guánica, Bahía de la Ballena, Puerto Rico (UPRRP 6381). The specimen measures 37.28 mm (SVL), and probably had reached its skeletal maturity and maximum size (Maisano, 2000; Regalado, 2006), based on the ossification of limb bones and the presence of parietals in contact along the midline of the skull.

Large isolated bones were photographed through the Leica MS5 dissecting microscope and the smaller ones through an Olympus BH-2 binocular phase contrast microscope. An average of 10 pictures for each bone was taken at different magnifications and depths. These pictures were combined with the multilayer focusing program CombineZ5.3 (Hadley, 2006). The braincase of a juvenile specimen of *Sphaerodactylus nicholsi*, a smaller species, was disarticulated, and each element was interpreted based on an articulated braincase of *S. roosevelti*.

Collection Acronyms

AMNH—American Museum of Natural History (New York, USA)

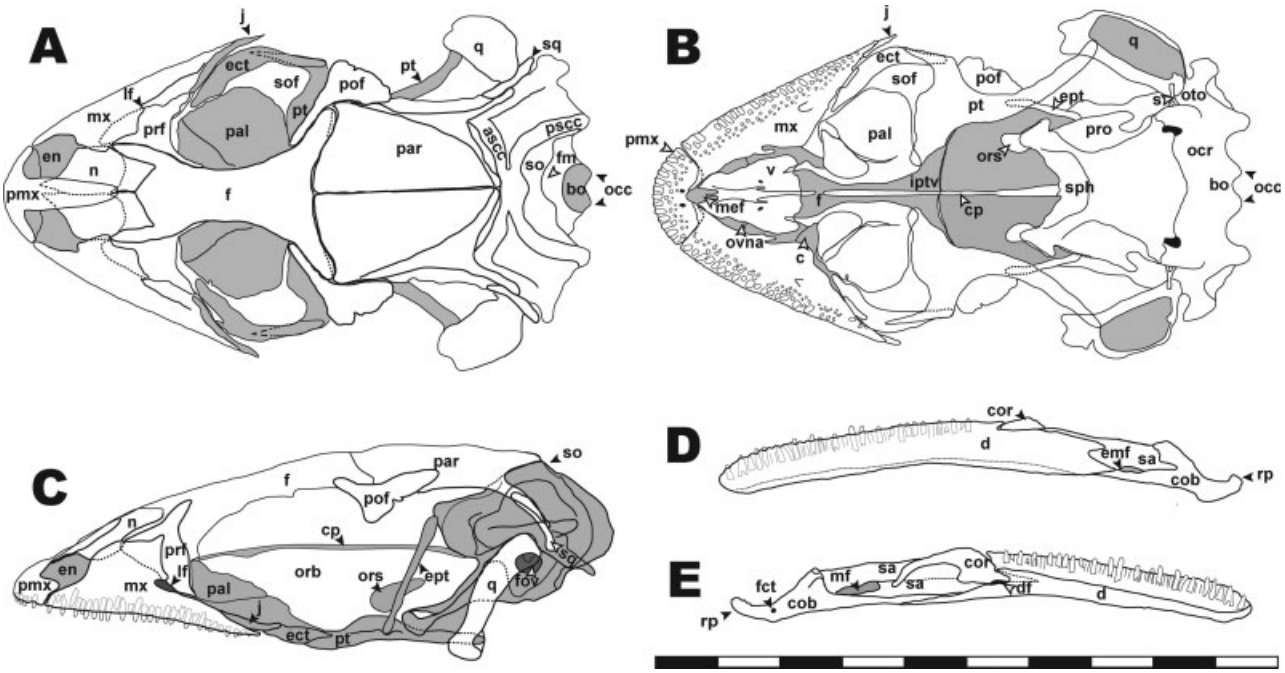

Fig. 2. *Sphaerodactylus roosevelti* (UPRRP 6381). Skull in (**A**) dorsal, (**B**) ventral, (**C**) lateral view, jaw in (**D**) lateral and (**E**) medial view. Scale bar = 10 mm. ascc, anterior semicircular canal; bo, basioccipital; c, choana; cob, compound bone; cor, coronoid; cp, cultriform process; d, dentary; df, dental foramen; ect, ectopterygoid; en, external nares; emf, external mandibular fenestra; ept, epipterygoid; f, frontal; fct, foramen for *chorda tympani*; fm, *foramen magnum*; fov, *fenestra ovalis*; iptv, interpterygoid vacuity; j, jugal; lf, lacrimal foramen; mef, medial foramen; mf, mandibular fossa; mx, maxilla; n, nasal; occ, occipital condyle; ocr, occipital recess, orb, orbit; ors, orbitosphenoid; oto, otooccipital; ovna, opening for the vomeronasal apparatus; pal, palatine; par, parietal; pmx, premaxilla; pof, postorbitofrontal; prf, prefrontal; pro, prootic; pscc, posterior semicircular canal; pt, pterygoid; q, quadrate; rp, retroarticular process; s, stapes; sa, surangular; so, supraoccipital; sof, suborbital fenestra; sph, sphenoid; sq, squamosal; v, vomer.

CM—Carnegie Museum of Natural History (Pittsburgh, USA)
FMNH—The Field Museum of Natural History (Chicago, USA)
MZSP—Museu de Zoologia da Universidade de São Paulo (São Paulo, Brazil)
UPRRP—Museo de Zoología, Universidad de Puerto Rico (San Juan, Puerto Rico)
YPM—Yale Peabody Museum of Natural History

RESULTS

Cranial Suture Patterns

Based on bone to bone contact, three types of sutures were identified in the skull of *S. roosevelti*: open contact sutures, overlapping sutures, and closed contact sutures. In the open contact suture or laminar suture (Evans and Klembara, 2005), the edges of the bones contact each other in juxtaposition, for instance the frontoparietal suture (Fig. 2A). A freely movable joint or diarthrosis is visible in the synovial palatobasal articulation between the sphenoid and pterygoid (Frazzetta, 1962). The overlapping sutures are similar to the *butt-lap* type of brazed joint in design. In this suture the bones contact each other in superposition, in which case the thickness of the bone is reduced by one-half in the contact area, and the edges are separated with one placed over the other. In the illustrations we show both bone edges, the one that lies below the other is drawn as a dashed line (e.g., Fig. 2A,C, where the maxilla overlaps the prefrontal and part of the maxilla overlaps the nasal laterally).

The closed contact suture is partly or totally invisible. In the following discussion we use closed contact rather than fused contact. The actual fusion of bone with bone (i.e., ankylosis of Romer, 1970) should be corroborated with X-rays or sections of the bones (Brochu, 1995). However, among some bones the fusion is so complete that no trace of a suture is visible, e.g. the otooccipital, which is the fusion of opisthotic and exoccipital (Bell et al., 2003; Montero et al., 2004).

Overall Description of the Skull and Jaw

The skull of the gekkotans is generally depressed and broad (Kluge, 1967). *S. roosevelti* has a skull with a wider snout than the other species from Puerto Rico and its skull roof is almost flat (Fig. 2A). The frontoparietal suture is curved and very wide, contrasting with the typically straight suture of "modern" lizards (Frazzetta, 1986), and the dorsal mesokinetic axis is highly movable. The oval external nares are visible and

placed anteriorly in the rostrum; they are separated by the ascending nasal process of the premaxilla and bordered posteriorly by the nasal and posterolaterally by the maxilla. The orbits occupy about 30% of the skull length; the orbit is oval and its longest axis is oriented anteromedially to posterolaterally, providing these geckos with a certain degree of binocularity. The orbit is not entirely surrounded by bone. It is delimited by the prefrontal anteriorly, the frontal medially, the jugal laterally, and the postorbitofrontal posterodorsally, being incomplete posteriorly. When the eye is removed, a D-shaped suborbital fenestra is visible (Fig. 2A), surrounded by the ectopterygoid laterally, the transverse process and palatine process of the pterygoid posteriorly, and the palatine anteromedially. In ventral view, the choanae are visible bordered posteriorly by the palatines and positioned posteriorly in the palate (c, Fig. 2B); the interpterygoid vacuity (= piriform recess, iptv, Fig. 2B) is wide posteriorly and narrow anteriorly, where the palatines approximate each other. The cultriform process of the sphenoid extends anteriorly approaching the vomer (cp, Fig. 2B). The occipital recesses are visible. The posterior margin of the semicircular canals extends further posteriorly than the occipital condyle.

In lateral view (Fig. 2C), the skull is wedge-shaped. The jugal lies over the maxilla and extends beyond it. The lacrimal foramen is bordered by the maxilla anteroventrally and by the prefrontal dorsolaterally with no participation of the jugal, a condition that differs from other geckos in which this foramen is usually located between the lateral part of the prefrontal and jugal; the maxilla may participate in the formation of its lateral margin (Rieppel, 1984c). The orbit is rounded and incomplete posteriorly. The fenestra ovalis lies posterior to the quadrate. In this view it is clear how the roof of the neurocranium (supraoccipital) comes to lie at the same level as that of the dermatocranium (parietal), closing the posttemporal fossae.

The mandible (Fig. 1D,E) is curved inward anteriorly. The dentary is the longest bone of the jaw with more or less parallel dorsal and ventral edges. In lateral view the low coronoid process is visible, forming an obtuse triangle. An external mandibular fenestra is visible in lateral view (emf, Fig. 2D), and is bordered by the surangular dorsally and the articular ventrally; this fenestra forms a lateral notch of the mandibular fossa (mf, Fig. 2E). In lingual view the dentary extends back to the level of the posteromedial process of the coronoid. The meckelian canal is closed, forming a fused dentary tube (Estes et al., 1988; Albino, 2005); it is continued from the dentary to the mandibular fossa. A medial opening, the dental foramen (df, Fig. 2E) is bordered by the dentary anteriorly. In UPRRP 6381, the anteromedial process of the coronoid inserts into the dentary at the level of the 28th tooth, contributing to the posterodorsal border of the dental foramen. In *Gonatodes* this process does not insert into the dentary tube. The dentary process of the surangular inserts into this tube as well, being situated between the dentary and the coronoid. The canal continues posteriorly between the surangular and the dentary and opens in the anterior part of the mandibular fossa. The mandibular fossa is bordered by the surangular anterodorsally and the compound bone ventrally. The foramen for the *chorda tympani* (fct, Figs. 1E and 7D) is visible at the base of the retroarticular process.

For seven adult specimens measured (four females and three males), the average adult skull length was 8.84 mm (8.49–9.29). In Puerto Rico, the smallest species is *S. nicholsi*, with an average adult skull length of 5.67 mm (5.29–6.15, two females and two males), a juvenile measured 4.00 mm. The dimensions of the skull illustrated are in Table 1.

Description of Isolated Bones

Dermatocranium

Premaxilla. This is an unpaired bone that contacts the maxilla posteroventrally, nasals posterodorsally, and vomer ventromedially. Although it bears 13 tooth loci, the specimen had only six functional teeth, some of which have a nutritive foramen. The teeth are isodont, cylindrical, pleurodont, and have rounded crowns. They probably have upright cusps, as has been reported for other sphaerodactyls (*Gonatodes albogularis, Sphaerodactylus nicholsi,* and *S. elegantulus*) using electron micrography (Sumida and Murphy, 1987). The bases of the teeth are medially swollen. The tooth positions are not evenly spaced, and most of the loci adjacent to functional teeth are empty or in a replacement state. On the cleared and stained specimen, a maximum of three rows of tooth buds are located at the base of each tooth both in the premaxilla and the maxilla. In dorsal and ventral view, the ascending nasal process (asnp, Fig. 3A) is arrowhead-shaped. The anterior part of the process has parallel margins, while the posterior half has margins that converge to form a rounded posterior end. This process overlaps the paired nasals (n-pmx, Fig. 3B) and reaches the frontal median process (fmp, Fig. 4A); nonetheless, there is no contact between the premaxilla and the frontal, because the nasals lie between them (Fig. 2A). The septonasal crest (snc, Fig. 3B) runs along the ascending nasal process ventrally. It has a medial swelling that lies between the anteriormost separation of the nasals. On the opposite side of this swelling, there is a shallow oval concavity (npc, Fig. 3A). The palatal process (plp, Fig. 3A,B) extends medially; its posteromedial area overlaps

TABLE 1. Measurements of the skull of Sphaerodactylus roosevelti (UPRRP 6381)

Measurement	Value (mm)	Description
Premaxilla length	1.85	From the anteriormost part of the premaxilla to the posterior end of the ascending nasal process
Skull length	9.27	From the anteriormost part of the premaxilla to the space between the divided occipital condyle
Width between the jugals	4.88	Measured between the posterior end of the jugals
Frontal posterior width	2.80	Measured at the posterior end of frontal
Width between the postorbitofrontals	4.22	Between the medial vertices of each postorbitofrontal
Left postorbitofrontal length	1.84	From the anterior process to the posterior process of the right postorbitofrontal
Skull greatest width	5.78	Between the most lateral part of the quadrates
Premaxilla width	1.50	From each premaxilla–maxilla suture
Left maxilla length	3.31	From the premaxilla–maxilla suture to the end of the posterior process of the maxilla
Occipital condyle width	0.43	Across the divided occipital condyle
Left orbit length	2.77	From the anteriormost margin of the orbit to the vertices of the postorbitofrontal
Highest point of the skull	3.37	From the mandibular condyle to the skull roof
Jaw length	8.40	From the mandibular symphysis to the posterior end of the retroarticular process of the left ramus
Height of the jaw	0.95	At the level of the coronoid
Jaw tooth row	4.39	Length of tooth-bearing portion of mandible

the premaxillary process of the maxilla, forming an overlapping suture (dashed line Fig. 2B). The palatal process forms the anterior edge of the medial foramen (mef, Fig. 2B). A longitudinal canal (lc, Fig. 3C) begins laterally at the base of the ascending nasal process and continues posteriorly, opening ventrally in the palatal process (polc, Fig. 3B).

Maxilla. This is a paired bone that contacts the premaxilla anteriorly, nasals anterodorsally, frontal dorsomedially, prefrontal posterodorsally, jugal posteromedially, ectopteryogoid and palatine medially. The right maxilla of the specimen UPRRP 6381 has only 16 functional teeth, but it bears 27 pleurodont tooth loci. The tooth row is straight. The teeth have the same morphology as those of the premaxilla, but the replacement is different. It is common to see two adjacent functional teeth, followed by one about to be shed. The replacement pattern in this species follows a typical Zahnreihe series (Edmund, 1969). The nutritive foramina of the teeth and several tooth buds are close to the medial shelf ventral surface (msh, Fig. 3F). The medial shelf extends medially, approaching the vomer and forming the lateral edge of the opening for the vomeronasal apparatus (ovna, Fig. 3F); it also forms the floor of the external naris anterodorsally and the anterolateral edge of the choana. The anterior premaxillary process (mxap, Fig. 3D–F) is an acute triangle with a 40° internal angle. Its area is almost fully overlapped by the posteromedial portion of the palatal process of the premaxilla. The superior dental foramen (sdf, Fig. 3F) is positioned at the junction of the shelf and the medial surface of the posterior dorsal process. The dorsal process is tall and roughly trapezoidal in outline. It slopes anteroventrally, bordering the external naris posterolaterally and the anterior margin of the lacrimal foramen. Both the anterior and posterior edges are nearly vertical, the posterior being the steepest and having the highest point as well. The dorsal process overlaps the nasal anterodorsally, and the prefrontal with which it has a lateromedial contact (Figs. 2C and 3E). The dorsal process has a septum that is small and partially separates the nasal from the prefrontal (mxs, Fig. 3E). The posterior process (mxpp, Fig. 3F) tapers posteriorly and is overlapped by the jugal.

Nasal. This is a paired bone, convex dorsally, with opposing edges roughly parallel to one another (Figs. 2A and 3G,H). It contacts the premaxilla anteromedially, maxilla laterally, septomaxilla ventrally, frontal posteriorly, has a small contact with the prefrontal laterally, and a medial contact with the other nasal. The anteromedial premaxillary process (apmx, Fig. 3G,H) bears a shelf facet contacting half of the ascending nasal process, which extends up to [3/4] of its medial length, up to the point where the nasal overlaps the frontal. In dorsal view, the area where the premaxilla lies is clearly visible (Fig. 3H). The anteromedial edge is emarginated and borders the posterior margin of the external naris. The posterior process (npp, Fig. 3G,H) overlaps the medial process of the frontal (fmp, Fig. 4A), covering it and the anterior emargination that connects this process with the lateral process of the frontal (flp, Fig. 4A). The dorsal process of the maxilla overlaps the laterodorsal surface of the nasal (n-mx, Fig. 3G). No foramina for the branches of the ophthalmic division of the trigemimal nerve and accompanying blood vessels were observed. The dorsal surface of the nasal shows some sculpturing. The contact

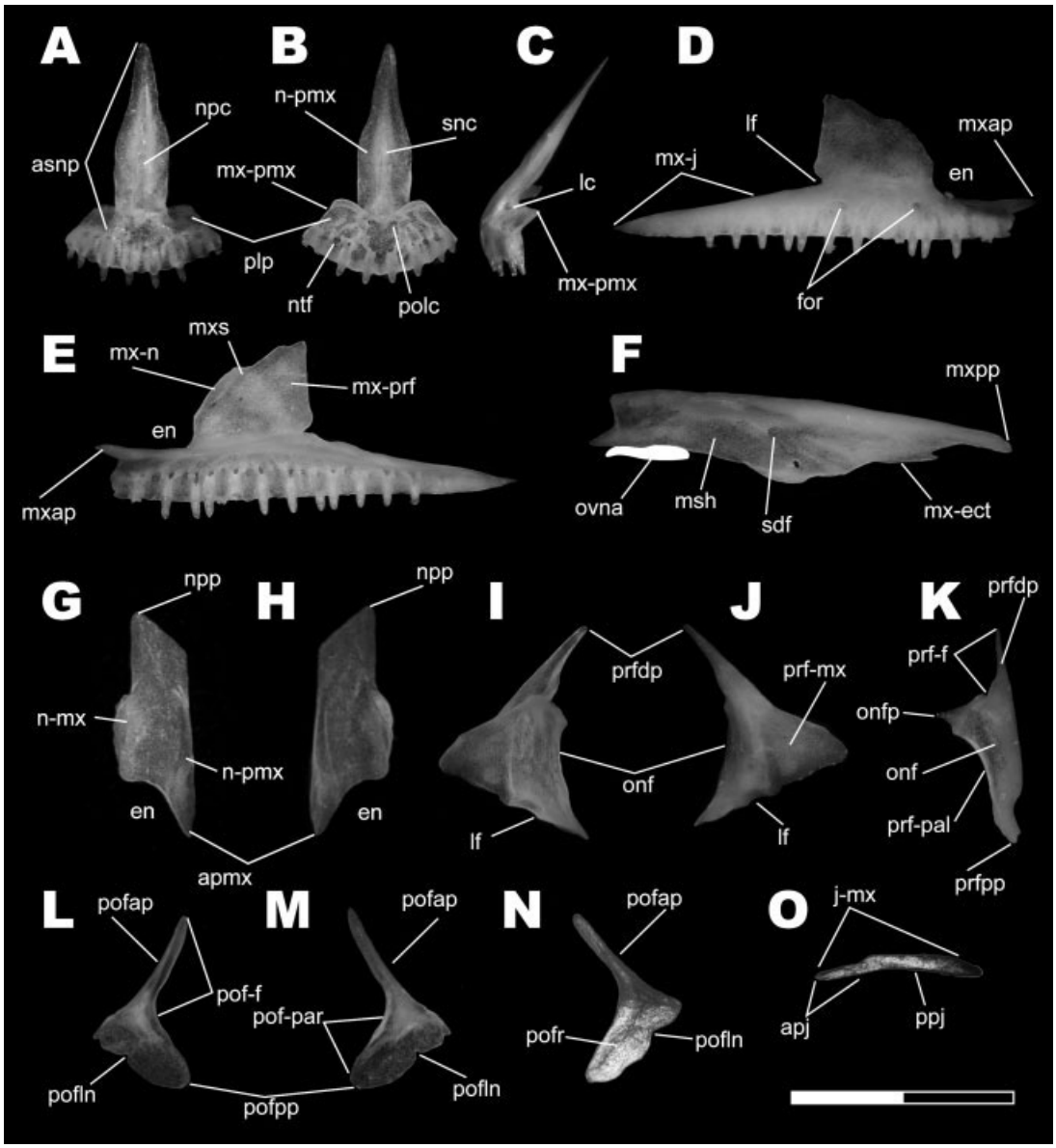

Fig. 3. *Sphaerodactylus roosevelti*. UPRRP 6487. **A**: Premaxilla anterodorsal view. **B**: Premaxilla posteroventral view. **C**: Premaxilla lateral view. **D**: Right maxilla lateral view. **E**: Right maxilla medial view. **F**: Right maxilla dorsal view. UPRRP 6490. **G**: Right nasal dorsal view. **H**: Right nasal ventral view. UPRRP 6487. **I**: Right prefrontal medial view. **J**: Right prefrontal lateral view. **K**: Right prefrontal posterior view. **L**: Right postorbitofrontal ventral view. **M**: Right postorbitofrontal dorsal view. UPRRP 6484. **N**: Right postorbitofrontal ventral view. UPRRP 6489. **O**: Right jugal dorsomedial view. Scale bar = 2 mm. apj, anterior process of jugal; apmx, anteromedial premaxillary process; asnp, ascending nasal process; en, external naris edge; for, foramina; j-mx, maxillary facet of jugal; lc, longitudinal canal; lf, lacrimal foramen; msh, medial shelf; mxap, anterior premaxillary process; mx-ect, ectopterygoid tab of the maxilla; mx-j, jugal facet of maxilla; mx-n, nasal facet of maxilla; mx-pmx, maxillary facet of premaxilla; mxpp, posterior process of maxilla; mx-prf, prefrontal facet of maxilla; mxs, septum of dorsal process of maxilla; n-mx, facet of dorsal process of maxilla; npc, ascending nasal process concavity; n-pmx, premaxillary facet of nasal; npp, posterior nasal process; ntf, nutritive foramen; onf, orbitonasal flange; onfp, orbitonasal flange projection; ovna, opening for the vomeronasal apparatus; plp, palatal process; pofap, anterior process of postorbitofrontal; pof-f, frontal facet of postorbitofrontal; pofln, postorbitofrontal lateral notch; pof-par, parietal facet of the postorbitofrontal; pofpp, posterior process of postorbitofrontal; pofr, postorbitofrontal ridge; polc, posterior opening of the longitudinal canal; ppj, posterior process of jugal; prfdp, dorsal process of prefrontal; prf-f, frontal facet of prefrontal; prf-mx, maxillary facet of prefrontal; prf-pal, palatine facet of prefrontal; prfpp, posterior process of prefrontal; sdf, superior dental foramen; snc, septonasal crest.

between the two nasals lies ventral to the skull surface. The ascending nasal process of the premaxilla overlaps them, leaving a small hollow space beneath it.

Prefrontal. This is a paired bone, triangular in outline. It contacts the maxilla, the frontal posterodorsally, and the palatine posteromedially. The contact between the posterior process of the pre-

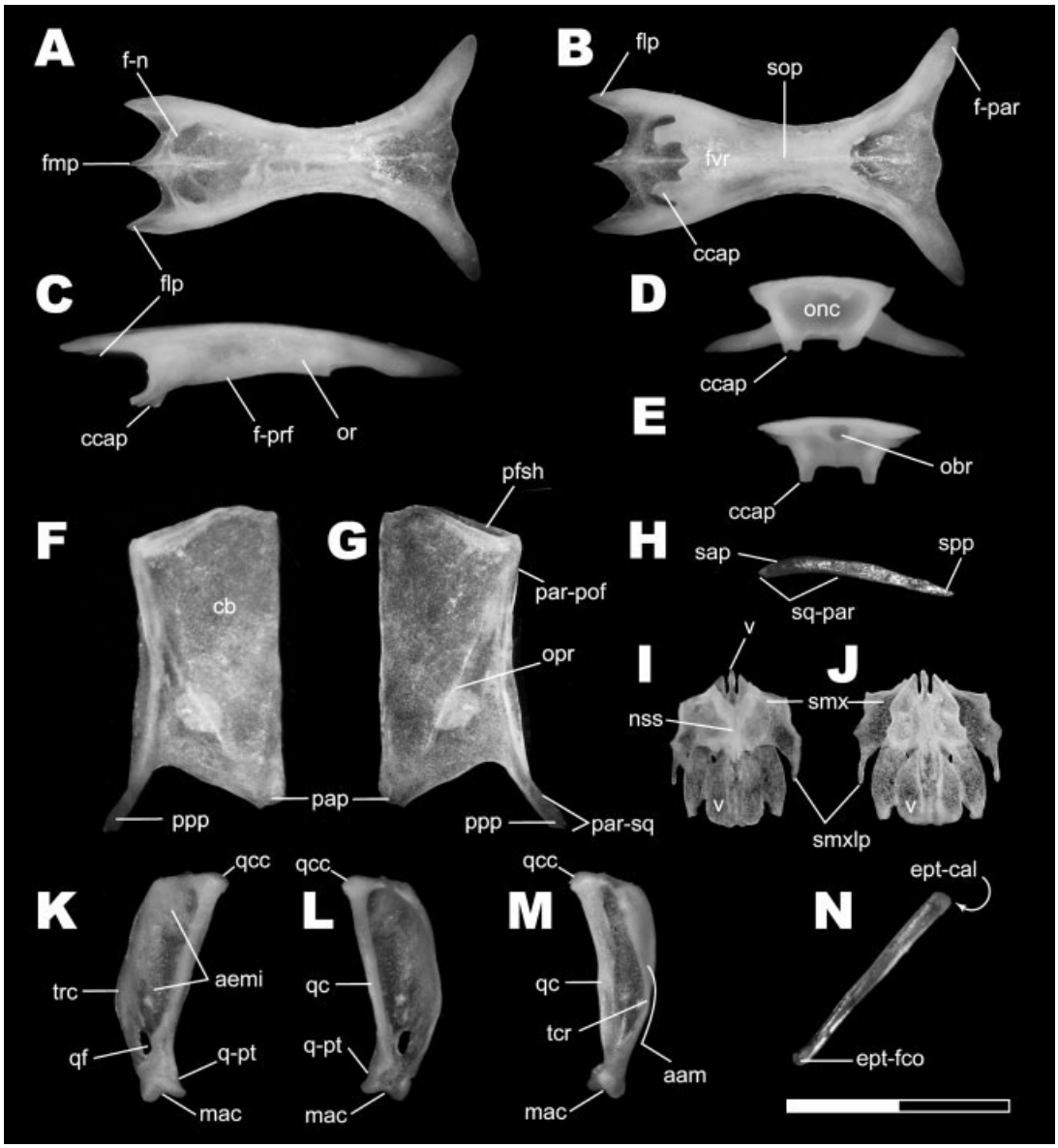

Fig. 4. *Sphaerodactylus roosevelti*. UPRRP 6484. **A**: Frontal dorsal view. **B**: Frontal ventral view. **C**: Frontal lateral view. **D**: Frontal anterior view. **E**: Frontal posterior view. **F**: Right parietal ventral view. **G**: Right parietal dorsal view. UPRRP 6489. **H**: Right squamosal. UPRRP 6484. Left and right septomaxilla articulated with vomer in (**I**) dorsal view and (**J**) ventral view. UPRRP 6490. **K**: Right quadrate anterior view. **L**: Right quadrate posterior view. **M**: Right quadrate posterolateral view. **O**: Right epipterygoid lateral view. Scale bar = 2 mm. aam, anterior edge of the auditory meatus; aemi, insertion of *m adductor externus mandibulae*; cb, concavity for the brain; ccap, anterior process of *crista cranii*; ept-cal, facet of epipterygoid for *crista alaris*; ept-fco, epipterygoid end that inserts in the *fossa collumellae*; flp, lateral process of frontal; fmp, medial process of frontal; f-n, nasal facet of frontal; f-par, parietal facet of frontal; f-prf, prefrontal facet of frontal; fvr, ventral ridge of frontal; mac, mandibular condyle; nss, nasal septum space; obr, opening for the braincase; onc, opening for the nasal cavity; opr, oblique parietal ridge; or, orbital ridge; pap, posteromedial process parietal; par-pof, postorbitofrontal facet of parietal; par-sq, squamosal facet of parietal; pfsh, parietal shelf for frontal; ppp, postparietal process; qc, medial column; qcc, cephalic condyle; qf, quadrate foramen; q-pt, pterygoid facet of quadrate; sap, anterior process of squamosal; smx, septomaxilla; smxlp, septomaxilla lateral process; sop, subolfactory processes; spp, posterior process of squamosal; sq-par, parietal facet of squamosal; tcr, tympanic crest; v, vomer.

frontal and the jugal varies inter and intraspecifically. The lateral surface has an overlapped suture with the posterior part of the dorsal process of the maxilla (prf-mx, Fig. 3J). The ventral edge is sinuous where it is overlapped by the maxilla, and it forms the posterodorsal margin of the lacrimal foramen. Posterior to this point the edge becomes straight and abuts the maxilla ventrally. The prefrontal curves posteromedially forming the orbitonasal flange (onf, Fig. 3I–K), which contacts the palatine medially and the frontal dorsally, keeping these two bones separated by a small projection

(onfp, Fig 3K). The dorsal process of the prefrontal (prfdp, Fig. 3I–K) is rod-like. It is directed anterodorsally and tapers gradually, contacting the descending process of frontal.

Postorbitofrontal. This is a paired bone, L-shaped in outline, having a 115° internal angle. It clasps the frontoparietal suture contacting the frontal anteromedially and the parietal posteromedially (Fig. 2A), forming a lateral brace for the movable frontoparietal suture (Rieppel, 1984c). The anterior process (pofap, Fig. 3L–N) is wide at the base and becomes strut-like but it does not taper, ending in a rounded tip. The end of the anterior process is firmly attached to the frontal, and the remaining contact with both the frontal and parietal is loose. The posterior process (pofpp, Fig. 3L–N) is 2.5 times broader than the anterior process and curves slightly dorsolaterally. The posterior process of the postorbitofrontal is more expanded than the anterior process in *Sphaerodactylus parkeri* from Jamaica (Stephenson, 1960). All the specimens examined present a lateral notch that varies from deep and narrow (pofln, Fig. 3L,M) to shallow and broad (pofln, Fig. 3N). There is no postorbitofrontal foramen (postfrontal foramina of Kluge, 1976).

Jugal. This is a paired, elongated, thin, strut-like bone resembling a Jai-Alai xistera (Figs. 2A and 3O). The anterior process is thinner, flaring out dorsally into the posterior process, which keeps a more or less constant width. Both ends are rounded. The jugal is dorsal to the maxilla and extends beyond the posterior margin of the maxilla. The posterior process of the jugal is partially suspended (ppj, Fig. 3O). The area of contact forms a butt-lap joint. Its main axis is obliquely oriented due to the curvature of the maxillary arcade. It also forms a diarthrosis with the medially adjacent ectopterygoid, which prevents a contact with the pterygoid flange. Contact of the jugal with the ventral process of the prefrontal is variable. In other gekkotans it has been described as being in contact (Häupl, 1980), almost in contact (Abdala, 1996), or separated. Among *Sphaerodactylus* the contact varies intra and interspecifically. The jugal does not participate in the lacrimal foramen in the *Sphaerodactylus* observed, but medially it borders a shallow groove that is a continuation of this foramen.

Frontal. This is an unpaired, hourglass-shaped bone that is overlapped by the nasals anteriorly. It has open contact sutures with the dorsal process of the prefrontal anterolaterally, palatines anteroventrally, postorbitofrontal posterolaterally, and parietals posteriorly. Dorsally a faint midline suture is visible, but this fades away midway along the bone. The suture is more evident anteriorly, where the medial process of the frontal is split (fmp, Fig. 4A). This division of the medial process reflects the initial pairing of the frontals in ontogeny. The two tips are asymmetrical in length, the left side being consistently longer in all specimens examined (n = 5). The lateral processes are slightly longer than the median process. The bone edges connecting these processes are emarginated. Each posterior nasal process overlaps half of the median process and the emarginated edge, leaving the lateral process exposed. The anterior end is roughly half the width of the posterior end. The latter is curved, and each posterolateral margin overlaps the parietals in a hinge-like articulation for the uplift of the muzzle unit. These areas of overlap are not as well defined as the frontal tabs seen in gymnophthalmids, and they are positioned at the posterolateral end (f-par, Fig. 4B). The *crista cranii* formed by the descending orbital ridges (or, Fig. 4C) and subolfactory processes (sop, Fig. 4B) (Montero et al., 2002; Bell et al., 2003) meet and fuse ventrally, forming a tubular structure bearing a ventral ridge (fvr, Fig. 4B = subolfactory crest Evans et al., 2004). This tube encases the olfactory tracts, and has a large kidney-shaped anterior opening for the nasal capsule (onc, Fig. 4D) and a posterior, rounded, smaller opening for the braincase (obr, Fig. 4E). The *crista cranii* has two anterior processes that have been described as two short pegs in *Sphaerodactylus* (nasal processes of Pregill, 1981). The orbital ridges are constricted in the middle of the orbit. The minimal interorbital width is 25% of the frontoparietal suture width.

Parietal. This is a paired element that contacts the frontal anteriorly, postorbitofrontal anterolaterally, prootic laterodorsally, squamosal posterolaterally, supraoccipital posteriorly, and the other parietal medially. With the frontal the two parietals form the relatively flat skull table. The parietal is subrectangular; the anterior edge is sigmoid and anterolaterally bears a small shelf that is overlapped by the frontal (pfsh, Fig. 4G). The posterior edge bears a 90° triangular emargination. The lateral "leg" of the triangle is a ventrally descending sliver of bone, the postparietal process (ppp, Fig. 4F,G), which has an extended lateral contact with the squamosal. The posteromedial process ends in an almost horizontal margin (pap, Fig. 4F,G). The median and lateral margins are almost parallel. Anterolaterally there is a straight edge, which is the articulation facet for the posterior process of the postorbitofrontal (par-pof, Fig. 4G). Ventrally it has a concavity accommodating one hemisphere of the cerebrum, optic lobe, and cerebellum (cb, Fig. 4F).

Squamosal. It contacts the postparietal process of the parietal dorsomedially (ppp, Fig. 4F,G) and roofs over the prootic and the otooccipital. It may contact the quadrate laterally. This bone plays only a minor role in quadrate suspension (Rieppel, 1984c). The posterior process is suspended (Fig. 2A), and its closer contact is with the parietal. In geckos, there is usually a ligamentous connection

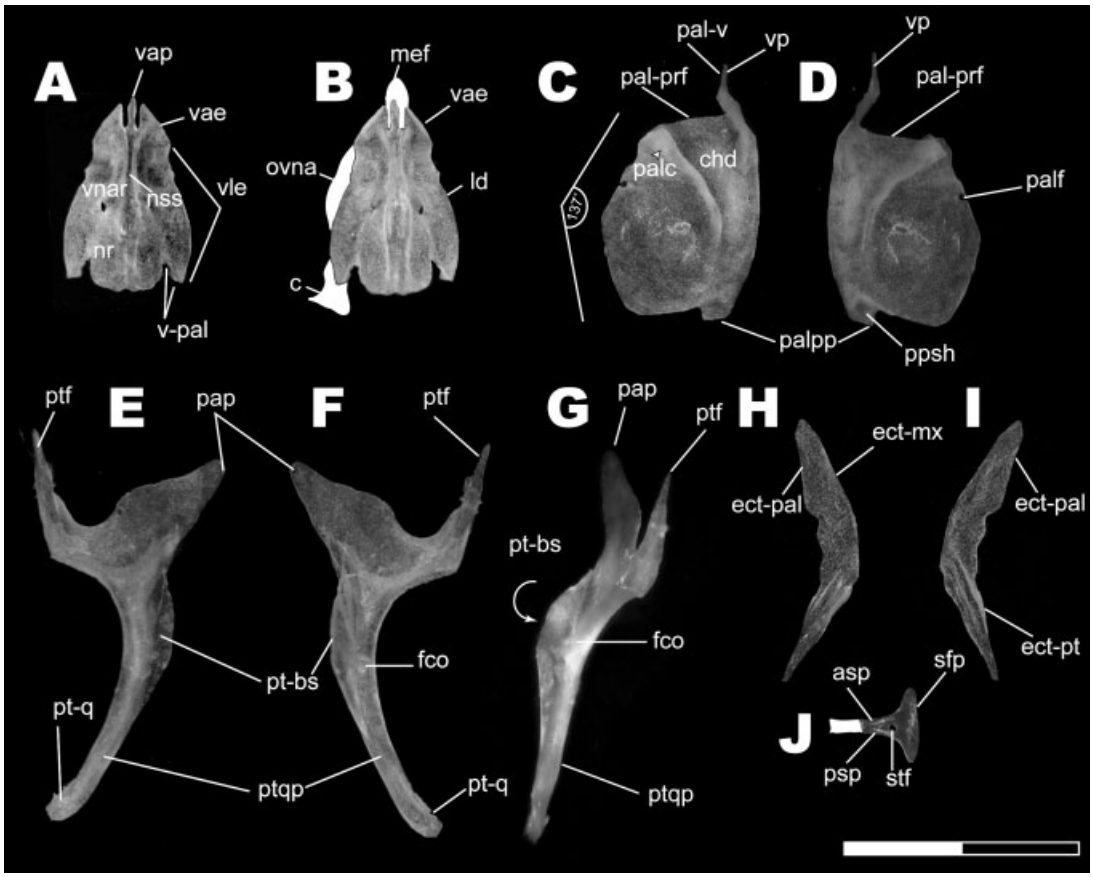

Fig. 5. *Sphaerodactylus roosevelti*. UPRRP 6484. **A**: Vomer dorsal view. **B**: Vomer ventral view. Solid white areas estimate the size of the openings bordered by vomer. UPRRP 6490. **C**: Right palatine ventral view. **D**: Right palatine dorsal view. **E**: Right pterygoid ventral view. **F**: Right pterygoid dorsal view. **G**: Right pterygoid lateral view. **H**: Right ectopterygoid dorsal view. **I**: Right ectopterygoid ventral view. Arrow indicates opposite side. UPRRP 6489. **J**: Right stapes ventral view. Scale bar = 2 mm. asp, anterior stapedial post; c, choana; chd, choanal duct; ect-mx, ectopterygoid depression that contacts the medial shelf of maxilla; ect-pal, ectopterygoid facet that contacts palatine; ect-pt, ectopterygoid facet that contacts lateral flange of pterygoid; fco, *fossa columellae*; ld, lacrimal duct opening; mef, medial foramen; nr, nasal region; nss, nasal septum space; ovna, opening for the vomeronasal apparatus; palc, ventral crest of palatine; palf, palatine foramen; palpp, pterygoid process of palatine; pal-prf, prefrontal facet of palatine; pal-v, vomerine facet of palatine; pap, palatine process of pterygoid; ppsh, shelf of palatine that contacts pterygoid; psp, posterior stapedial post; pt-bs, facet of pterygoid that contacts basipterygoid; ptf, pterygoid flange; pt-q, facet of pterygoid that contacts quadrate; ptqp, quadrate process of pterygoid; sfp, stapes footplate; stf, stapedial foramen; vae, anterolateral edge of vomer; vap, anterior process of vomer; vle, lateral edge of vomer; vnar, vomeronasal region; vp, vomerine process; v-pal, vomerine facet that contacts palatine.

between the cephalic condyle of the quadrate (qcc, Fig. 4K–M) and the squamosal (Rieppel, 1984c). This connection was not observed in *S. roosevelti* but is very conspicuous in *Quedenfeldtia trachyblephara* (Fig. 9B).

Septomaxilla (Turbinal of Wellborn, 1933). The septomaxilla is a paired bone that covers the vomeronasal apparatus dorsally (syn. organ of Jacobson) as in most squamates (Bernstein, 1999). In lateral view, the space occupied by the vomeronasal apparatus (syn. *concha vomeronasalis*) is visible. Its dorsal surface forms the anterior part of the nasal capsule. The space between the bones is filled by the nasal septum cartilage (nss, Fig. 4I). The lateral process (smxlp, Fig. 4I,J) abuts the maxillary surface medially.

Vomer. This is an unpaired (i.e., fused), laminar bone. It contacts the premaxilla and maxilla anteriorly, the septomaxilla dorsally, and palatine posteriorly. It forms the central roof of the mouth along with the palatal process of the premaxilla (plp, Fig. 3A,B) and the maxillary medial shelf (msh, Fig. 3F). The anterior edge is W-shaped, forming the posterior border of the medial foramen (mef, Figs. 2B and 5B), also referred to as the incisive foramen (Liang and Wang, 1973). The anterior vomerine process (vap, Fig. 5A) divides the medial foramen posteriorly. The length of this process is variable; in *S. roosevelti* it may or may not exceed the length of the anterolateral edge (e.g., Figs. 2B and 5A,B). In *Gonatodes* it is very short, and it is absent in *Coleodactylus* and *Lepidoblepharis*. The anterolateral

edge of the vomer (vae, Fig. 5A,B) contacts the premaxilla–maxilla suture (Fig. 2B). The lateral edge (vle, Fig. 5A) forms the medial edge of the opening for the vomeronasal apparatus (ovna, Fig. 5B). Posteriorly it forms the anteromedial edge of the choana (Häupl, 1980). The posterior end is notched, having a small shelf for the vomerine process of the palatine (v-pal, Fig. 5A). The dorsal surface has the vomeronasal and the nasal regions, but no septum is visible (vnar and nr, Fig. 5A). The space for the nasal septum and the articulation of septomaxilla is visible (nss, Fig. 5A). We interpret the paired foramina in the middle part of the bone as the lacrimal ducts (ld, Fig. 5B), because they are posterior to the end of the septomaxilla in the nasal region.

Palatine. This is a paired element that contacts the vomer anteriorly, prefrontal anterodorsally, pterygoid posteriorly, maxilla and ectopterygoid laterally. The bone is squarish with convex lateral flanges. It forms the posterior border of the choana and the anteromedial border of the suborbital fenestra (ic and sof, Fig. 2A,B). Anteriorly it has a foot-like vomerine process (vp, Fig. 5C,D) that overlaps the vomer, a type of suture with a marked reduction of contact that was described as hypokinetic (Rieppel, 1984c) and reflects the development of a high degree of cranial kinesis. The anterior edge curves downward, contacting the orbitonasal flange of the prefrontal (onf, Fig. 3K). The pterygoid process (palpp, Fig. 5C,D) is three times shorter and three times broader than the vomerine process. Dorsally it bears a shelf that receives the palatine process of the pterygoid (ppsh, Fig. 5D), forming a tongue-in-groove articulation (Bell et al., 2003). The posterolateral adjacent edge is flat and straight, bordering a slit that extends medially from the suborbital fenestra. The lateral edge has an angular projection (137°) midway along its length. There is a notch anterior to the vertex of this angle, which in some specimens may complete a bony connection and appear as a foramen. We interpret this notch/foramen as the palatine foramen (palf, Fig. 5D), which carries nerves and blood vessels. The ectopterygoid has an open contact suture with the palatine at the adjacent sides of the palatine foramen. The anterolateral edge is separated from the medial shelf of the maxilla, but it is possible that these two bones may contact during cranial kinesis. In ventral view, there is a prominent crest (palc, Fig. 5C) that runs almost diagonally and demarcates a smooth, concave surface that continues the choana, prolonging the choanal duct (chd, Fig. 5C) toward the midline. In dorsal view, the surface is flat. The medial edge is suspended and borders the anterior portion of the interpterygoid vacuity. The orbitonasal flange projection of the prefrontal prevents the contact between the two short pegs of the *crista cranii* and the palatine.

Pterygoid. This is the largest bone of the skull. It is paired, Y-shaped, and contacts the palatine and ectopterygoid anteriorly, the epipterygoid dorsally, the sphenoid medially, and the quadrate lateroposteriorly. The anterior edge is sinuously indented, making the bone roughly Y-shaped. The palatine process is broad and rounded, and the pterygoid flange is acute (pap and ptf in that order, Fig. 5E,G), resulting in a movable articulation with the palatine, and a stiffer articulation with the ectopterygoid. Next to the palatine process, the anterior edge is straight and forms the posterior border of the slit that extends medially from the suborbital fenestra. Lateral to this slit, the pterygoid edge is markedly concave, defining the characteristic D-shaped suborbital fenestra of the sphaerodactylines and *Pristurus* (see Fig. 9). Lateral to the concavity, the bone projects anteriorly to form the acuminate pterygoid flange. This flange does not contact the jugal or the maxilla. The quadrate process (ptqp, Fig. 5E–G) curves laterally, originating behind the *fossa columellae* (fco, Fig. 5F) which accommodates the base of the epipterygoid bone. This process contacts the posteromedial edge of the quadrate. The knob-like process of the pterygoid is absent. This, when present, contacts the basipterygoid at maximum retraction and thereby effectively increases the tendency of the pterygoids to spread apart (Frazzetta, 1962). In the cleared and stained specimens, the basipterygoid processes of the sphenoid and the basipterygoid facet of the pterygoid are well separated; the synovial palatobasal articulation contains the cartilaginous meniscus pterygoidii.

The pterygoid has a flattened area that contacts the basipterygoid (pt-bs, Fig. 5E–G), this feature together with the absence of the knob-like process indicates that the basisphenoid-pterygoid articulation is weak.

Ectopterygoid. This is a paired, crescent-shaped bone that contacts the maxilla anterolaterally, palatine anteromedially, and pterygoid posteriorly. The anterior end separates the palatine and maxillary medial shelf posteriorly and excludes the maxilla from the suborbital fenestra. On the dorsal surface there is a small depression for the tab of the maxillary medial shelf (ect-mx, Fig. 5H). The posterior end has a triangular ventral groove that overlaps the pterygoid flange (ect-pt, Fig. 5I). This end is wider than the pterygoid flange and prevents a contact between the pterygoid and the maxilla. In lateral view the bone curves downward, since the palate is positioned at a higher level than the pterygoid. The contact with the pterygoid is exclusively ventral, in contrast to other species where this bone forms both a dorsal and ventral process for the support of the pterygoid flange (Kluge, 1962).

Splanchnocranium. The articular bone, which is also part of the splanchnocranium, is discussed with the other bones of the jaw (see below).

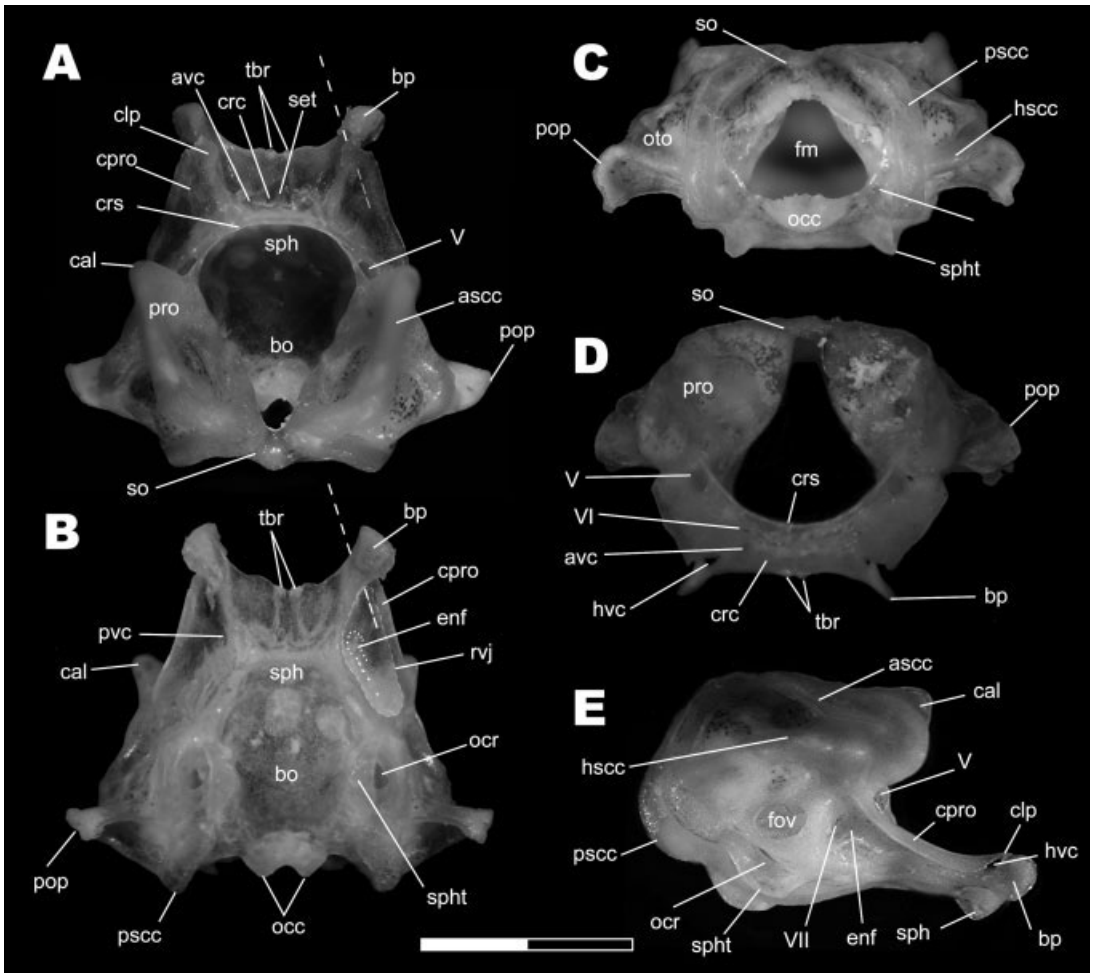

Fig. 6. Basicranium of *Sphaerodactylus roosevelti*. UPRRP 6490. **A**: Dorsal view. **B**: Ventral view. **C**: Posterior view. **D**: Anterior view. **E**: Lateral view. Scale bar = 2 mm. ascc, anterior semicircular canal; avc, anterior opening of vidian canal; bo, basioccipital; bp, basipterygoid process; cal, *crista alaris*; clp, clinoid process; cpro, crista prootica; crc, carotid canal; crs, *crista sellae*; enf, entocarotid fossa; fm, foramen magnum; fov, *fenestra ovalis*; hscc, horizontal semicircular canal; hvc, groove for the course of the lateral head vein; occ, double occipital condyle; ocr, occipital recess; oto, otooccipital; pop, paroccipital process; pro, prootic; pscc, posterior semicircular canal; pvc, posterior opening of vidian canal; rvj, *recessus vena jugularis*; set, *sella turcica*; so, supraoccipital; sph, sphenoid; spht, sphenooccipital tubercle; tbr, trabeculae, V, *incisura prootica* for the course of the trigeminal nerve; VI, abducens canal; VII, facial foramen.

Epipterygoid. This is a columnar bone, tilted posteriorly, and forming a 67° angle with the horizontal quadrate process of the pterygoid and extending from the pterygoid *fossa columellae* (fco, Fig. 5F,G) to the *crista alaris* of the prootic (cal, Fig. 6A,B,E). Its dorsal end is slightly wider and flatter than the ventral end.

Quadrate. The quadrate is a large, lightly built shell-like bone with a large posterior concavity. It contacts the squamosal dorsally, otooccipital dorsomedially, pterygoid posteromedially, and the articular ventrally. The bone has a convex smooth anterior surface. Part of the space that is produced by the concavity of the quadrate forms the auditory meatus, which in sphaerodactyls has no muscles for its closure (Wever, 1973). The cephalic condyle is positioned dorsomedially (qcc, Fig. 4K–M), contacting the paroccipital process of the otooccipital (exoccipital + opisthotic) in suspension by "paroccipital abutting" (Rieppel, 1984c). There is a medial column (qc, Fig. 4L,M) extending between the cephalic and mandibular condyles. The mandibular condyle is concave and appears as two distal condyles (mac, Fig. 4K–M). The base of the condyle is constricted where it contacts the pterygoid. The dorsal surface of the quadrate slopes slightly downward, then makes a sharp bend, turning almost vertical at the tympanic crest (tcr, Fig. 4K,M). The tympanic crest is not enlarged, but projects anteriorly where it outlines the anterior edge of the auditory meatus (aam, Fig. 4M), and the union of the tympanic membrane. On the anterior surface, above the mandibular condyle, there is a large oval foramen (qf, Fig. 4K).

Stapes. In combination with the cartilaginous extrastapes, this bone forms the *columella auris*. The oval footplate (sfp, Fig. 5J) fits into the fenestra ovalis. Two posts originate from the footplate, one anterior and other posterior (asp and psp in that order, Fig. 5J); they meet laterally, forming an internal angle of 26°. The arches are united by a lamina that is perforated by the stapedial foramen (stf, Fig. 5J), which is the passageway of the stapedial artery (Rieppel, 1984c).

Neurocranium. The braincase, as in most lizards, is divided in an orbitotemporal region represented by the paired orbitosphenoids and the otooccipital region that is formed by the sphenoid, basioccipital, supraoccipital, prootic, and otooccipital (Bever et al., 2005).

Otooccipital region. This region forms the basicranium, a solid structure formed by the fusion of three medial unpaired elements (sphenoid, basioccipital, and supraoccipital) and two lateral paired elements (prootic and otooccipital). This compound structure is covered by the parietals dorsally, and articulates with the quadrates, pterygoids, epipterygoids, and the vertebral column.

In skeletally mature specimens of *S. roosevelti*, the fusion of the sphenoid and basioccipital is complete, although in some specimens the suture is better defined, which indicates that fusion was ongoing. In all the immature specimens examined, the chondrocranial basisphenoid and the dermatocranial parasphenoid were fused into the sphenoid, which seems to occur early in development. The brain space is cone-shaped, with a maximum width dorsally (Fig. 6A). The prootics and the supraoccipital form two internal sloping walls, reducing the space toward the bottom, but this space expands close to the base where the basioccipital and the sphenoid form a concave surface. The foramen magnum (fm, Fig. 6C,D) is triangular, occupying a large portion of the rear part of the skull. It is bounded by the supraoccipital dorsally, the otooccipitals lateroventrally, and ventromedially by the basioccipital (Fig. 6C). The occipital condyle is double (Gardiner, 1982). It is formed by the otooccipitals (exoccipitals) laterally and basioccipital medially. Additionally, a hypocentral element of the proatlas is added to the occipital condyle making the craniovertebral (occipito-atlantal) joint intravertebral and intersegmental (Kamal, 1961). The inner ear cavities are complex and bounded by the prootic, supraoccipital, and otooccipital. Inside these cavities, there is a large amount of calcified endolymph, which in some specimens is confluent with the endolymph of extracranial endolymphatic sacs. These sacs are connected to the sacculus of the inner ear.

Sphenoid. This is a compound bone resulting from the fusion of the basisphenoid and the parasphenoid. It contacts the prootic dorsally, the basioccipital posteriorly, and participates in the synovial palatobasal articulation with the pterygoids (Frazzetta, 1962). Anteriorly it bears the paired *trabeculae* (trb, Figs. 6A,B,D and 7A), from which a cartilaginous rod or cultriform process (= trabecula comunis) originates. This process extends anteriorly, close to the posterior edge of the vomer. In juveniles, the trabecula is more well-defined than in the adult. The trabeculae are rounded transversely, and converge in orientation, while in the adult, these are parallel. The basipterygoid processes (bp, Figs. 6A,B,D,E and 7A,B) are oriented anterolaterally, with the distal facets covered by cartilage in both juveniles and adults. Dorsal to the basipterygoid processes is a groove for the course of the lateral head vein (hvc, Fig. 6E). This groove is covered dorsally by the clinoid process of the sphenoid (clp, Fig. 6A,E). The clinoid process is well developed and elongated. It originates from the *crista sellae* (= *dorsum sellae*) and runs parallel on the dorsal surface of the basipterygoid process. The lateral edge of the clinoid process is straight and diagonally oriented, contacting the *crista prootica* of the prootic (cpro, Fig. 6A).

In dorsal view the *sella turcica* is visible (set, Figs. 6A and 7B), and is delimited by the *crista trabecularis* and the *crista sellae* (cts and crs in that order, Fig. 7B). It accommodates the hypophysis. Laterally to the *sella turcica* and lying at the same level are the paired carotid canals (crc. Fig 6A = internal carotid) and next to them the anterior openings of the Vidian canal (avc, Figs. 6A and 7B). The posterior opening of this canal opens posterolaterally on the ventral surface of the sphenoid (pvc, Figs. 6B and 7A), which indicates that the canal is oriented obliquely. Dorsolaterally to the carotid canal is located the abducens canal for the course of cranial nerve VI (Fig. 6D)

Basioccipital. This is a shield-shaped bone that underlies a large part of the posterior part of the brain. It contacts the sphenoid anteriorly, otooccipital laterally and the vertebral column (atlas). The suture with the sphenoid is very faint in adults following fusion. This bone forms the medial portion of the double occipital condyle, and the middle part of the ventral edge of the *foramen magnum*. The basioccipital is prevented from contributing to the lateral edge of the *occipital recess* (ocr, Figs. 2B,6B, and 7C) by a slender splint of bone from the otooccipital, but it participates in the formation of a low sphenooccipital tubercle (spht, Fig. 6B,E), which in sphaerodactylines, *Pristurus*, *Quedenfeldtia*, and *Teratoscincus* does not cover the *recessus scalae tympani* in ventral view.

Prootic. This irregularly shaped bone forms the anterodorsal part of the basicranium. It contacts the sphenoid anteroventrally, epipterygoid anterolaterally, supraoccipital posterodorsally, and the otooccipital posteroventrally. The dorsal surface of the prootic is flat, a character state scored

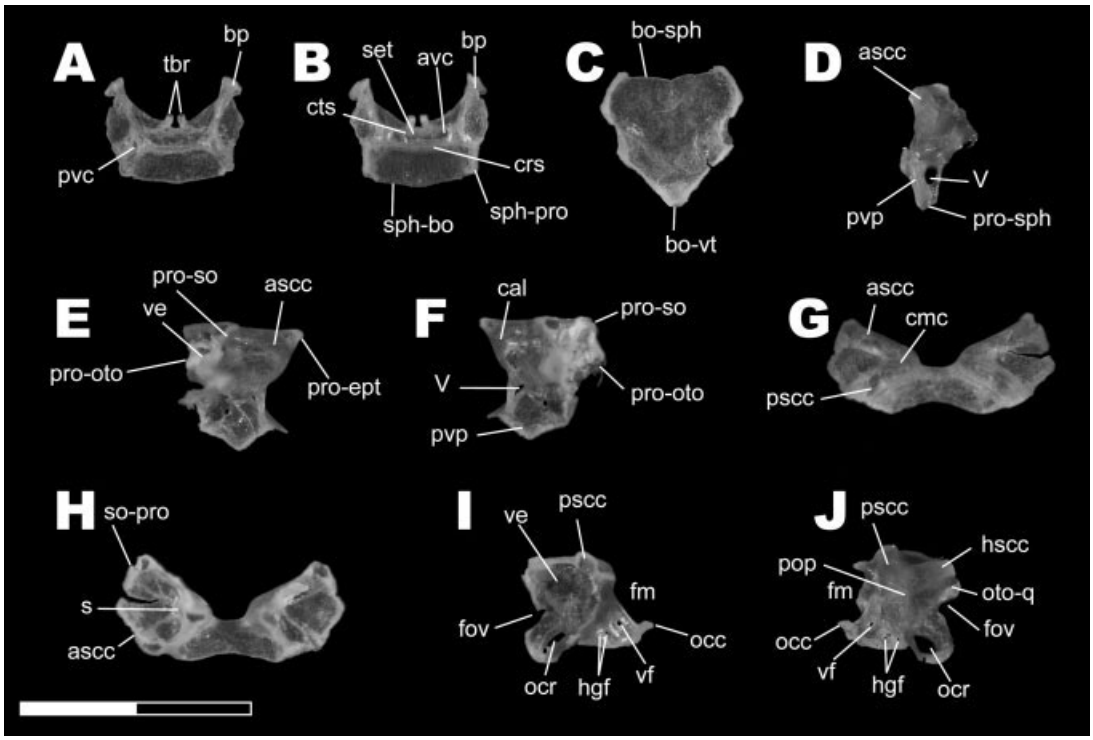

Fig. 7. Juvenile of *Sphaerodactylus nicholsi*. **A**: Sphenoid ventral view. **B**: Sphenoid dorsal view. **C**: Basioccipital dorsal view. **D**: Prootic frontal view. **E**: Prootic lateral view. **F**: Prootic medial view. **G**: Supraoccipital dorsal view. **H**: Supraoccipital ventral view. **I**: Otooccipital posteromedial view. **J**: Otooccipital posterolateral view. Scale bar = 2 mm. ascc, anterior semicircular canal; avc, anterior opening of vidian canal; bo-sph, sphenoid facet of basioccipital; bo-vt, basioccipital facet that contacts vertebrae; bp, basipterygoid process; cal, *crista alaris*; cmc, common crus; crs, *crista sellae*; cts, *crista trabecularis*; fm, foramen magnum; fov, fenestra ovalis; hgf, hypoglossal foramen; hscc, horizontal semicircular canal; occ, occipital condyle; ocr, occipital recess; oto-q, quadrate facet of otooccipital; pop, paroccipital process; pro-ept, epipterygoid facet of prootic; pro-oto, otooccipital facet of prootic; pro-so, supraoccipital facet of prootic; pro-sph, sphenoid facet of prootic; pscc, posterior semicircular canal; pvc, posterior opening of vidian canal; pvp, prootic ventral process; st, septum; set, *sella turcica*; so-pro, prootic facet of supraoccipital; sph-bo, sphenoid facet for basioccipital; sph-pro, sphenoid facet for prootic; trb, trabeculae; ve, vestibule; vf, vagus foramen; V, *incisura prootica* for the course of the trigeminal nerve.

for sphaerodactyls and some other gekkonoids (Grismer, 1988). In none of the cleared and stained specimens was the prootic in contact with the parietal, although posterior contact may occur in life. This bone houses the anterior part of the membranous labyrinth (Kluge, 1962). Together with the otooccipital, it houses the inner ear. It also forms the anterior margin of the *fenestra ovalis* (fov, Fig. 2C). The most prominent part of the prootic is the *crista alaris* (cal, Figs. 6A,B,E and 7F), which bears two enlarged ridges or ampullar bulges, the tracks of the anterior and horizontal semicircular canals (ascc, Fig. 7E) (Jollie, 1960). The anterior portion of the *crista alaris* has a projecting point that braces the dorsal end of the epipterygoid (Grismer, 1988; pro-ept, Fig. 7E). The vertical ventral process (pars trigeminalis of Kluge, 1962) (pvp, Fig. 7D,F) originates below the *crista alaris* from the ampullar ridge. This process is pierced anteroposteriorly by the incisura prootica for the course of the trigeminal nerve (V, Figs. 6A,E and 7D,F).

The ventral process of the prootic flares out anterolaterally, forming the *crista prootica*. The *crista prootica* contacts the lateral edge of the clinoid process of the sphenoid and forms the roof for the *recessus vena jugularis* (rvj, Fig. 6B). The entocarotid fossa (enf, Fig. 6B) appears as a shallow groove within the *recesus vena jugularis* and is exclusively derived from the prootic with no participation of the sphenoid. At the end of this fossa, in the suture with the otooccipital, is the facial foramen for the course of cranial nerve VII (Fig. 6E).

Supraoccipital. This is a butterfly-shaped bone, which forms the posterodorsal margin of the basicranium. It contacts the prootic anteriorly, and the otooccipitals ventrally, bordering the *foramen magnum* dorsally. On the dorsal surface two enlarged ridges are visible: the anterior one, which is a continuation of the ampullar ridge of the prootic, roofs the anterior semicircular canal (ascc, Fig. 7G); the posterior ridge roofs the posterior semicircular canal (pscc, Fig. 7G) and continues onto the otooccipital. These are confluent in the common crus

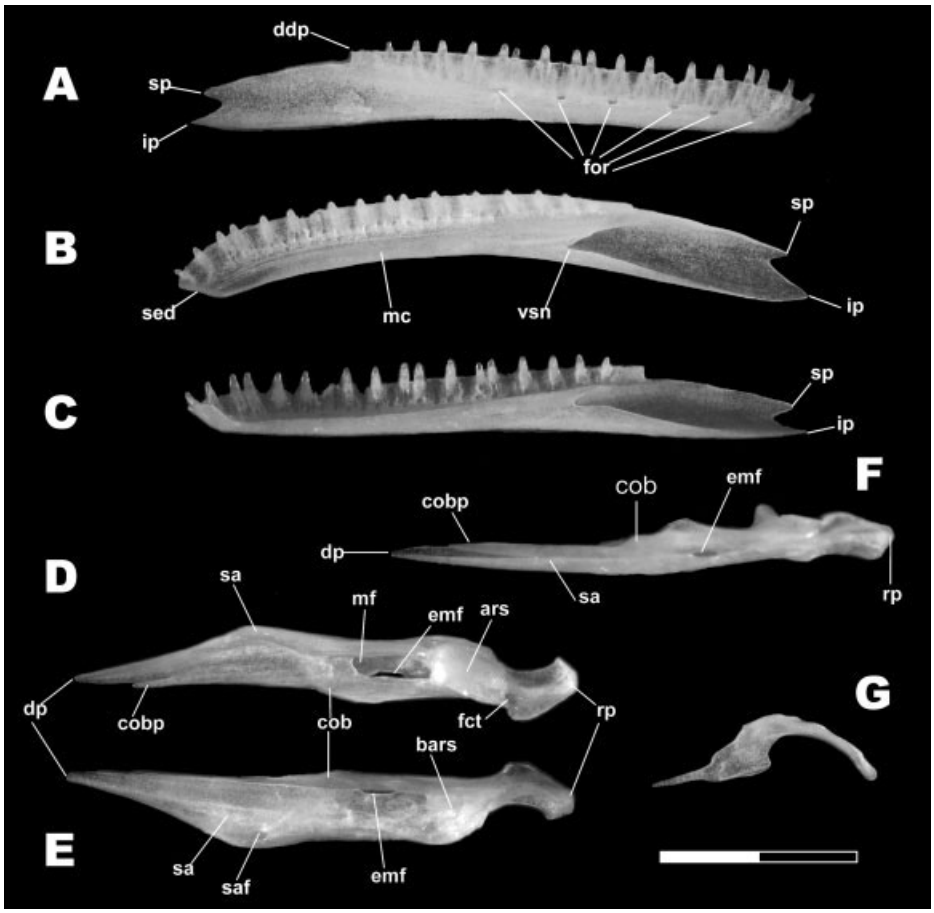

Fig. 8. *Sphaerodactylus roosevelti*. UPRRP 6490. **A**: Dentary medial view. **B**: Dentary dorsal view. **C**: Dentary lateral view. **D**: Surangular and compound bone medial view. **E**: Surangular and compound bone lateral view. **F**: Surangular and compound bone ventral view. **G**: Coronoid lateral view. Scale bar = 2 mm. ars, articular surface; bars, anterolateral brace for the articular surface; cap, anterior process of coronoid; cob, compound bone; cobp, anterior process of compound bone; ddp, dorsal process of dentary; cpp, posterior process of coronoid; crp, coronoid process; dp, dentary process; emf, external mandibular fenestra; fct, foramen for *chorda tympani*; for, foramina; ip, inferior process; mc, meckelian canal; mf, mandibular fossa; rp, retroarticular process; sa, surangular; saf, foramen carrying cutaneous branches of the inferior alveolar nerve; sed, symphiseal edge; sp, superior process; vsn, v-shaped notch.

(cmc, Fig. 7G). The two canals are partially divided by a bony septum (st, Fig. 7H). In ventral view all the cavities formed by the dorsal bulging are full of calcified endolymph. The small endolymphatic foramen was not visible.

Otooccipital. This is an irregularly shaped bone that forms the posterolateral portion of the braincase. It contacts the prootic anteriorly, basioccipital ventromedially, supraoccipital dorsally, quadrate laterally, and the parietal dorsolaterally. In posterolateral view the horizontal semicircular canal is visible (hscc, Figs. 6C,E and 7J). It runs from the intersection with the posterior semicircular canal (pscc, Figs. 6B,C and 7I) along the lateral surface until it reaches the prootic. The *occipital recess* (ocr, Fig. 7I,J) is rectangular with rounded edges and is located ventral to the *fenestra ovalis*. This recess is completely surrounded by the otooccipital with no participation of the basioccipital. Posterior to the *occipital recess*, there are three small foramina; we interpret two of them as hypoglossal foramina (hgf, Fig. 7I,J) because they are completely within the exoccipital of the otooccipital. The larger one is the vagus foramen (vf, Fig. 7I,J), which marks the original separation of the opisthotic and exoccipital (Bever et al., 2005).

Mandible

Dentary. The dentary is a tubular bone with the Meckelian canal closed (Rivero-Blanco, 1976; Estes et al., 1988; Albino, 2005). It contacts the coronoid and the surangular posteriorly. It constitutes most of the length of the mandibular ramus and is slightly curved anteriorly (Figs. 2D,E and 8A,B). It bears 17 isodont, cylindrical, pleurodont teeth with rounded crowns. The teeth appear well spaced, because the alternate teeth are frequently lost, but the maximum number of tooth loci in the right ramus is 30. The lateral side is flattened and has

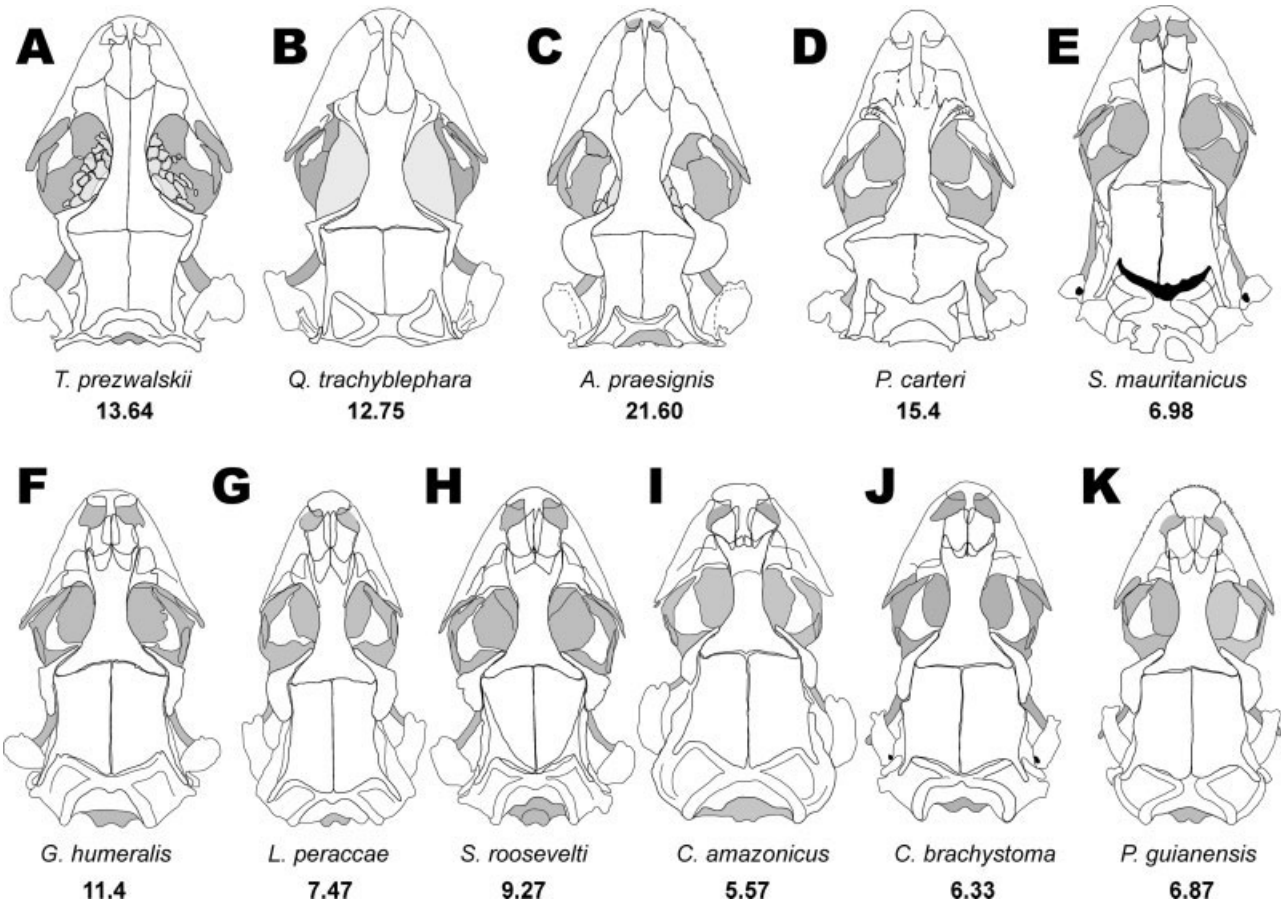

Fig. 9. Dorsal view of 11 sphaerodactylid geckos. Numbers below drawings are total skull length in millimeters. E–K, miniaturized forms.

seven mental foramina (for, Fig. 8A). The dorsal edge of the postdental part develops a small dorsal process (ddp, Fig. 8A,C) that can be vertically or obliquely oriented. This postdental region extends posteriorly, forming the superior and posterior processes (sp and ip in that order, Fig. 8A–C), the former shorter than latter. The symphyseal edge (sed, Fig. 8B,C) is slender and obliquely oriented. The Meckelian canal begins anterior to a flat surface behind the symphysis and becomes progressively broader, opening in a V-shaped notch at the level of the 27th tooth. The anterior coronoid process and the dentary process of the surangular are inserted into the Meckelian canal. The dentary forms the ventral edge of the dental foramen (df, Fig. 2E) at the beginning of this notch.

Coronoid. This is a sickle-shaped bone that contacts the dentary anteriorly, the surangular and the compound bone posteriorly. The anterior process (cap, Fig. 8G) has a rounded tip and has more or less parallel dorsal and ventral edges. It expands into a plate three times its width at the base of the coronoid process (crp, Fig. 8G). From the coronoid process the posterior process curves downward, contacting the compound bone.

Surangular + compound bone. In skeletally mature specimens, the fusion of surangular and the compound bone is incomplete. The suture between them is visible and there is some movement possible between elements, but in the rear part fusion is complete. In a juvenile specimen of *S. nicholsi* these two bones were completely separated. Because of their fusion in adults, we describe these bones together. The surangular (sa, Fig. 8D–F) is a massive bone that lies over the compound bone (cob, Fig. 8D–F); it forms the anterodorsal edge of the mandibular fossa (mf, Figs. 2E and 8D) and the lateral edge of the external mandibular fenestra (emf, Figs. 2D and 8D–F). It has an acute dentary process (dp, Fig. 8D–F) that surpasses the anterior process of the compound bone. Posteriorly it develops an anterolateral brace for the articular surface (bars, Fig. 8E). On the dorsolateral surface it has a large foramen that carries the cutaneous branches of the inferior alveolar nerve (saf, Fig. 8E). The surangular is con-

cave. With the compound bone it forms an extension of the Meckelian canal to the mandibular fossa. The compound bone is long and forms the posteroventral part of the jaw, participates in the craniomandibular articulation, and forms the medial edge of the external mandibular fenestra. This bone is probably the fusion of three bones, the articular, prearticular, and angular. This fusion takes place early in development or shortly after hatching, since in the juveniles examined it is already fused. The articular surface (ars, Fig. 8D) is rectangular, bearing a medial ridge and two low depressions that accommodate the concave mandibular condyle of the quadrate (mac, Fig. 4K–M). The posterior part is formed by the retroarticular process, which is flat and relatively open (Häupl, 1980). The foramen for the *chorda tympani* (fct, Fig. 8D) is located on the medial side, where the retroarticular process begins.

DISCUSSION

Skull Bones

In his definition of the muzzle unit, Frazzetta (1962) neglected to mention the frontal bone, but this unit includes the premaxilla, nasals, paired septomaxillae, vomer, maxillae, prefrontals, frontal, lacrimals, and the anterior portion of the palatines. Another name used in reference to the muzzle unit is palatomaxillary unit (Herrel et al., 1999), in which the frontal and the palatines are included but not the septomaxilla. The gekkotan muzzle unit differs from that defined by Frazzetta because of the loss of the lacrimals and the integration of the jugal. The jugal overlies the maxilla. As a consequence it moves with the rest of the muzzle unit when the mouth opens.

Overlapping sutures or butt-lap joints are common among the bones of the muzzle unit. Stephenson (1962) discussed the overlapping in the muzzle region of the skull and the differential extension of the ascending nasal process of the premaxillae in the snake-like pygopodids (his prenasal process of the premaxillae). He described *Aprasia* as having a minor separation of the nasals anteriorly, *Pygopus*, *Delma,* and *Lialis* with a variable separation between [1/4] and [1/2] the length of the nasals, and *Pletholax* with completely separated nasals. This variation was later described by Kluge (1976) in an explicit discussion of characters. However he did not make a distinction between an anterior separation of the nasals by the laminar contact with the premaxilla or the apparent separation of these bones caused by the overlap of the premaxilla. For example in *S. roosevelti*, the nasals are only slightly separated anteriorly, but due to the overlying ascending nasal process of the premaxilla, their contact cannot be seen (Fig. 2A). In some gekkotans the nasals are separated by the edge of the ascending nasal process. Others have the nasals separated, and the edge of nasal process of the premaxilla lies over them. For example in *S. roosevelti*, superficially the nasals seem to be separated by the ascending nasal process of the premaxilla, but these two bones are in contact along almost their entire length, being separated just at the anterior end (Fig. 2A). In dorsal view the separation of the nasals looks larger due to the overlapping suture with the premaxilla. In many lepidosaurs the nasal bones do not meet anteriorly, which seems to be a widespread condition that probably appeared in some of the early amniotes from the Late Carboniferous (Early Pennsylvanian) (Carroll and Baird, 1972; Carroll, 1988a,b,1991). It is possible that when this character originated, the separation of nasals was due to an open contact suture with the posterior edge of the ascending nasal process. In gekkotan species with broad ascending nasal processes, like sphaerodactyls or the pygopodids *Delma*, *Pygopus,* and *Pletholax,* the overlapped suture is obvious. In species with a narrow ascending nasal process, like *Aprasia* and *Lialis* it is more complicated to tell if they have an abutting suture or if they overlap. For example, when examined under the contrast microscope, some gekkonoids with a similar narrow ascending nasal process (e.g., *Phyllodactylus wirshingi*, *Hemidactylus angulatus*, and *H. brooki*), show overlapping and the anterior separation of the nasals. In all the sphaerodactyls the premaxilla overlaps the nasals. The overlap is [1/4] to [1/2] of the nasal length in *Gonatodes,* around [1/2] in *Lepidoblepharis*, between [1/2] and [3/4] in *Sphaerodactylus*, and complete separation in *Coleodactylus amazonicus*, where the ascending nasal process is longer and contacts the frontal. The skull length of the specimen of *C. amazonicus* (MZSP 67239) was 5.38 mm, this being the smallest skull found among the adult sphaerodactyls studied. It is possible that complete separation of nasals is a characteristic only found in an extremely miniaturized skull. In *C. amazonicus* the rostrum is shorter than in *Sphaerodactylus* and the nasal bones are triangular and small.

In the Gekkota, the single element that clasps the frontoparietal suture is referred as the postfrontal by the majority of authors, which assumes a complete loss of the postorbital (Camp, 1923; Wellborn, 1933; Stephenson, 1960; Häupl, 1980; Estes et al., 1988; Gao and Norell, 2000). This identification is based on the fact that the bone that clasps the frontoparietal suture in squamates is commonly the postfrontal (de Beer, 1937), although there are some exceptions reported (e.g., *Python argus*) where it is the postorbital (McDowell and Bogert, 1954). In the oldest reported gekkonomorph, AMNH FR21444, the postfrontal and the postorbital are separated (Conrad and Norell, 2006) and the postfrontal has an L-shape as in many gekkotans. Since the postorbital and post-

frontal have different shapes and contacts, one can often discriminate them on those bases alone. By that criterion, the single element in gekkotans is the postfrontal, which unlike the postorbital, wraps around the frontoparietal suture (Jacques Gauthier, personal communication). Some authors assume a fusion of the postorbital and the postfrontal and may refer to this bone either as the postorbitofrontal (Rieppel, 1984c; Abdala, 1996) or as the postfrontal only (Kluge, 1967, 1976). Prenatal and postnatal studies have not shown separate centers of ossification for these two bones in limbed gekkotans (El-Toubi and Kamal, 1961; Bellairs and Kamal, 1981; Maisano, 2000). In the pygopodid *Lialis jicari,* Rieppel (1984c) reported two separated rudiments of bone in the area of the postorbitofrontal. In pygopodids there is a single element. This is frequently divided by a foramen, the postorbitofrontal foramen of Kluge (1976). Since pygopodids are nested within Gekkota as the sister taxon of the Diplodactylidae or Carphodactylidae (Kluge, 1987; Donnellan et al., 1999; Han et al., 2004, but see Röll and Henkel, 2002), this suggests that the single bone of more basal gekkotans might be composite (Susan Evans, personal communication).The absence of the postorbital or its fusion to the postfrontal has been treated in several cladistic analyses of Squamata (Estes et al., 1988; Evans and Barbadillo, 1998; Lee, 1998; Conrad, 2008), being coded differently in each study. Estes et al. (1988) scored the postfrontal as present for Gekkonidae and Pygopodidae, separated from the postorbital or absent for Gekkonidae and dubious for Pygopodidae. The postorbital was scored as present for both Gekkonidae and Pygopodidae. Lee scored his character 24 (Postfrontal, [0] remains separate from postorbital throughout ontogeny; [1] fusing with postorbital during ontogeny) as not applicable to Gekkota, while he scored the postorbital as absent (his character 27). Evans and Barbadillo scored the postfrontal as separated from the postorbital and the postorbital absent. The term postorbitofrontal assumes fusion of the postorbital and the postfrontal. Whether the postorbital really contributes to this element or not is open to discussion, but considering the current evidence and the ambiguity of this character from the previous cladistic analyses, it is best to use the term postorbitofrontal. The validity of this name will be tested as new information about the ontogeny of gekkotans becomes available. Based on recent cladograms (Lee, 1998; Townsend et al., 2004; Conrad, 2008), this compound bone has developed independently several times in other squamates like the Scincidae, Lacertiformes, Anguidae, Xenosauridae, and Varanidae.

The jugal in some gekkotans is reduced or lost, as in some pygopodids (McDowell and Bogert, 1954; Kluge, 1976; Estes, 1983). In sphaerodactyls the jugal is always present, and the shape is variable. For example in *Gonatodes* it is flattened while in *Sphaerodactylus* it is more rounded. The gekkonomorph AMNH FR21444 differs from the gekkotans in the possession of a complete postorbital bar where the jugal abuts the postfrontal (Conrad and Norell, 2006). This is also present in *Myrmecodaptria microphagosa* from Upper Cretaceous of Ukhaa Tolgod, Mongolia (Gao and Norell, 2000), but this animal is an extremely odd and robustly built form of questionable affinity (Evans, 2003a). In a recent analysis it appeared outside of the Gekkonomorpha as the sister taxa of *Ardeosaurus* + Autarchoglossa (Conrad and Norell, 2006). In all gekkotans the postorbital bar is incomplete and does not abut the postorbitofrontal. This character was defined as a synapomorphy of Gekkota (Estes et al., 1988).

The nasal lies over a shelf facet in the frontal which is separated from the other nasal by a narrow ridge, similar to the situation in the gymnophthalmid *Neusticurus ecpleopus* (Bell et al., 2003), and in a lesser extent the pythonomorph *Coniasaurus* (Caldwell, 1999).

In all gekkotans, the *crista cranii* of the frontal fuse ventrally (McDowell and Bogert, 1954; Underwood, 1957; Stephenson, 1960; Kluge, 1967; Estes, 1983; Estes et al., 1988) forming the tubular *canalis olfactorius* (1973); this is convergent with some gymnophthalmids. Our results show that in *S. roosevelti* a ridge is visible at the junction of the subolfactory processes (fvr, Fig. 4B), contrary to the morphology described for the gekkotans in which fusion is complete without leaving any trace of a suture (Rieppel, 1984c). In AMNH FR21444, the *crista cranii* is not fused ventrally, but all gekkotans including *Gobekko* (Conrad and Norell, 2006) and *Hoburogekko* (Alifanov, 1989, 2000) possess a frontal bone fused ventrally, indicating that this feature appeared in the gekkotan evolution at least during the Early Cretaceous.

In all the sphaerodactyls we found an unpaired frontal. In some gekkotan genera these are paired or unfused (Bauer, 1990a; Kluge and Nussbaum, 1995; Abdala, 1996), which has been suggested to be secondarily derived from the fused condition by paedomorphic retention of an embryonic stage (Kluge, 1967). Among sphaerodactylids, paired frontals were found in *Teratoscincus prezwalski* and *Saurodactylus mauritanicus* (Fig. 9A,E).

Two *Sphaerodactylus* fossil frontals have been recovered from the Late Pleistocene in the Blackbone 1 cave (located 1.2 Km due south of Iglesia Ascensión, Ciales, Puerto Rico) (Pregill, 1981). The bones measured 2.3 and 2.5 mm in length. The *S. roosevelti* specimens reviewed have frontal bones above 3.69 mm. If the fossil material represents species with skeletal maturity, this would rule out two of the six species currently inhabiting Puerto Rico (i.e., *S. roosevelti* and *S. klauberi*). This material should be re-examined and compared with the

isolated bones of the other four species in order to try to identify these fossils.

The parafrontal ossifications (Bauer and Russell, 1989), identified as a putative synapomorphy for *Aristelliger* and *Teratoscincus* (Gamble et al., 2008a) could not be verified in other geckos. It is unlikely that these ossifications are present in miniaturized sphaerodactylids, since in all of them the eye bulges out from the skull in dorsal profile. In cleared and stained preparations of *Quedenfeldtia trachyblephara* we found a continuous mesenchymal sheet lying at the same level of the frontal bone and extending from the postorbitofrontal to the prefrontal bone (Fig. 9B). This structure is probably homologous with the one found in *Aristelliger* and *Teratoscincus*, and might correspond to a synapomorphy of that clade of large sphaerodactylids (see Fig. 1); it remains to be corroborated in *Euleptes*.

In the Squamata the parietal bone is paired early in ontogeny and typically fuses to form a single element (Kluge, 1967). In many geckos these two bones remain separated throughout their life. Paired parietals among geckos have been interpreted as a paedomorphic feature (Stephenson, 1960; Kluge, 1967). Kluge interpreted this widespread character of gekkotans as derived from the primitive fused parietals of eublepharines and the fossil Ardeosauridae. At that time Ardeosauridae was considered basal among the Gekkota (Camp, 1923; Hoffstetter, 1962, 1964; Estes, 1983). In currently cladistic analysis *Ardeosaurus* and *Bavarisaurus*, formerly placed among the Gekkota (Estes, 1983), are outside of it (Conrad and Norell, 2006). Recent studies recovered *Ardeosaurus* as the sister taxon of the crown group Autarchoglossa and *Scandensia*, *Eichstaettisaurus*, and *Bavarisaurus* as three consecutive outgroups of Scleroglossa (Conrad and Norell, 2006). In another analysis *Eichstaettisaurus* was found to be the sister taxa of a clade form by *Hoyalacerta* and *Parviraptor* (Evans and Wang, 2005), but a more comprehensive recent analysis suggests that *Eichstaettisaurus* is a basal scincogekkonomorph (Conrad, 2008).

Paired parietals are present in the Lower Cretaceous gekkonomorphs AMNH FR21444 (Conrad and Norell, 2006) and *Hoburogecko* (Alifanov, 1989, 2000) and the Late Cretaceous *Gobekko* (Borsuk-Białynicka, 1990). The posterior emargination of the parietal (see Fig. 9) was proposed as a synapomorphy for sphaerodactyls by Grismer (1988), a trait that he also found to be present in *Teratoscincus*, *Aristelliger* and *Pristurus,* genera now included in the Sphaerodactylidae. This emargination is totally absent in some geckos (e.g., *Nephrurus*), in which the parietal process is also shorter.

In most gekkotans there is a single bone in the temporal region. The identity of this bone has been debated extensively. Originally it was identified as the quadratojugal (Baur, 1889). In a later revision of the temporal region of squamates, Camp (1923) concluded that this single bone in geckos was the tabular. His conclusion was influenced by reasoning that the reduction of the squamosal must have accompanied the reduction of the arches. He also mentioned that in some geckos a rudimentary element, half the size of the tabular was present. He identified it as the squamosal. Underwood (1957) refuted this interpretation, and based on observations of *Aeluroscalabotes* and *Hemitheconyx*, he concluded that the tiny inner bone was the supratemporal (= tabular), and the outer element was the squamosal. Kluge (1967) agreed with Underwood, supporting this identification with evidence for the loss of supratemporal in some eublepharid geckos (Kluge, 1962). In gekkotan morphological descriptions, three names have been used, probably for the same homologous bone: supratemporal (Stephenson, 1960; Fabián-Beurmann et al., 1980), temporal (Häupl, 1980), or squamosal (Wellborn, 1933; Kluge, 1962; Rivero-Blanco, 1976; Abdala, 1996). In *S. roosevelti*, as in the majority of gekkonid lizards, there is only one bone, which we refer to as the squamosal. The squamosal of scleroglossans lacks its dorsal process (Estes et al., 1988), and is described as hockey-stick shaped (Rieppel, 1994). In the sphaerodactyls the squamosal is straighter, departing from this generalized form. The squamosal is lost in *Teratoscincus prezwalskii*, *Saurodactylus mauritanicus*, *Lepidoblepharis peraccae*, and *Coleodactylus amazonicus* (Fig. 9A,E,G,I).

A dorsally expanded, convex septomaxilla reflects an enlarged Jacobson's organ and is a synapomophy of the Scleroglossa (Estes et al., 1988). In iguanids, agamids, and chamaeleonids the vomeronasal apparatus is often reduced apparently due to the diminished importance of olfactory stimuli in the arboreal habitat (Pratt, 1948; Hallermann, 1994; Bernstein, 1999). For example in the iguanian *Pristidactylus* the vomeronasal apparatus is poorly developed and the septomaxillae are small and flat (Montero et al., 2004). On the other hand, field observations showed that a terrestrial iguanian, *Sceloporus jarrovi*, shows much higher frequency of tongue extensions than the arboreal *Anolis trinitatis*, which suggests that terrestrial iguanians may be better able to use chemical cues to detect their terrestrial predators and prey (Gravelle, 1980). Evidence from nasal capsule, brain, tongue, and behavior has been presented to support the idea that geckos are olfactory specialists, with a tongue-vomeronasal system not remarkably advanced over the presumed ancestral condition exemplified by some iguanids (Schwenk, 1993). *S. roosevelti* shows a further development of the vomeronasal apparatus covered by a convex septomaxilla. Its tongue has a complex structure with multiple longitudinal bundles (Schwenk, 1988) and a tip notched with smooth margins. All

of this in addition to its terrestrial habits indicates some vomeronasal olfaction capabilities, perhaps to a lesser degree than the pygopodid vomeronasal apparatus-harderian gland association (Rehorek et al., 2000). Sphaerodactyls also have the fovea shifted to a temporal position, which makes possible binocular fixation, an obvious advantage to visual prey detection (Underwood, 1954).

The vomer among gekkotans has been identified incorrectly as the prevomer (Kluge, 1962; Liang and Wang, 1973). Kluge mentioned the relation between a rostral process(es) of the prevomer (i.e., anterior process of the vomer) and the prevomerine process (es) of the premaxilla, which in some species overlap or abut. In these cases the medial foramen is divided into two portions. In *Coleonyx variegatus* (YPM 14383 Maisano, 2003a), two oval foramina are visible, which appear as a broader medial foramen divided by a wide partition. Kluge (1995) scored the maxillae of *Sphaerodactylus* as separated or in narrow contact posterior to the premaxilla. In *S. roosevelti* the maxillae are well separated. The premaxilla overlaps the maxilla medially. This is why the vomer contacts these two bones simultaneously at the maxilla–premaxilla suture. This condition is widespread among the sphaerodactyls. In an earlier work Kluge (1987) discussed how the anteromaxillary shelf of the maxilla tends to separate the vomer and the premaxilla, a condition present in agamids, chamaeleonids, geckos, and some basal pygopodids.

The anterodorsal surface of the quadrate in *S. roosevelti* is smooth and not keeled, contrary to what has been reported for *S. goniorhynchus* and other gekkonids (Grismer, 1988).

The occurrence of the stapedial foramen is considered primitive in reptiles (Underwood, 1957) and has been reported in some gekkonids, *Dibamus*, and *Anelytropsis* (Kamal, 1961; Greer, 1976; Rieppel, 1984a; Bauer, 1990b). In sphaerodactyls, the stapedial foramen shows minor individual variation (Kluge, 1987) but is almost always present. The absence of closure muscles at the auditory meatus has been inferred to be a consequence of being mute. Because of that, sphaerodactyls would not need to "protect" themselves against their own vocalizations (Wever, 1973). From the ear morphology seen in *S. roosevelti* we cannot support or reject this idea; future behavioral research will add information to determine whether or not these animals vocalize.

In geckos, the orbitotemporal region is more reduced in older animals than in younger ones (Kamal, 1961). In embryos this region comprises the *pila metoptica*, *pila antotica*, and *pila accessoria*, the latter two having been reported as missing in fully formed chondrocrania of geckos (Kamal, 1961). Two small, drop-shaped bones are visible in lateral view of the *S. roosevelti* skull, which are ossifications of the pila metoptica (Bellairs and Kamal, 1981). We interpret these as the orbitosphenoids. These bones are positioned dorsal to the basipterygoid process of the sphenoid, and medial to the epipterygoid, just behind the orbit. Beyond their presence we cannot provide further morphological details from the cleared and stained specimens, because these small bones are barely visible using the available optical microscopes. Because of the small size of these bones, they are lost or overlooked in standard skeletal preparations (Bever et al., 2005). Some cartilaginous structures may be associated with these bones.

In recent cladistic analysis (Conrad and Norell, 2006; Conrad, 2008) a character in which the *occipital recess* is either visible in ventral view or hidden by the spheno-occipital tubercle is described. *Gonatodes*, *Teratoscincus,* and *Coleonyx* were coded as having a visible *occipital recess*. This character should include an intermediate state where the *occipital recess* is partially hidden by the sphenooccipital tubercle, which is the condition in the eublepharids such as *Coleonyx* and *Eublepharis*.

Jollie (1960) distinguished geckos and pygopodids in three ways: having the anterior margin of the prootic nearly straight thereby lacking a trigeminal notch (*incisura prootica*) because it is fully enclosed (V, Figs. 6A,E and 7D,F), having a ventral anterior process of the prootic, and having the posterior clinoid process of the sphenoid (basisphenoid). The presence of a fully enclosed trigeminal "notch" is common among gekkonomorphs, for example it is present in the Early Cretaceous gekkonomorph AMNH FR21444 (Conrad and Norell, 2006). In a small survey we found it in the eublepharids *Eublepharis macularius* and *Hemitheconyx caudicinctus,* the carphodactylid *Nephrurus levis,* the gekkonids *Gehyra oceanica, Hemidactylus haitianus, Phelsuma lineata, Saltuarius cornutus, Thecadactylus rapidauda*, and in the sphaerodactylids including *Aristelliger lar* and *Teratoscincus microlepis*. This notch was not found in *Gekko gecko,* which has a highly modified *crista alaris* and in the pygopodids *Delma molleri*, *Lialis burtonis*, *Pygopus lepidopodus*, and *Pygopus nigriceps*. In the pygopodids the *crista alaris* is absent and the *crista prootica* is elongated anteroposteriorly, producing an emarginated anterior margin of prootic. In *S. roosevelti* we did not observe a supratrigeminal process in front of the *incisura prootica* as it is in the gekkonomorph AMNH FR21444.

The presence of extracranial endolymphatic sacs filled with calcified endolymph is not constant in sphaerodactyls. In a sample of 69 cleared and stained *Sphaerodactylus* from six species, we found that approximately three out of four animals have extracranially hypertrophied endolymphatic sacs. In females these sacs are three times more frequent than in males. Males predominate among the specimens with no visible sacs. These sacs

have been interpreted as reservoirs of calcium for egg formation (Bustard, 1968), storage of calcium for yolk production (Bauer, 1989), and orientation and equilibrium for arboreal lizards (Moody, 1983). In geckos of the genus *Eurydactyloides* it was suggested that they could play a role in periods of rapid growth and bone formation (Bauer, 1989). Likewise, in the amphisbaenian *Amphisbaena darwini* it was suggested that they play an important role during ossification of the skeletal system or may be involved in adult calcium metabolism (Mangione and Montero, 2001). Given that hypertrophied sacs are present in female, males, juveniles, and hatchlings of sphaerodactyls, we are inclined to the latter explanation.

In one juvenile of *S. nicholsi* we observed complete fusion of the opisthotic and exoccipital, and we identified the vagus foramen which marks their original separation (Bever et al., 2005). In juveniles, these two bones fuse into the otooccipital probably shortly after hatching or birth (Maisano, 2001). This fusion has been proposed as a synapomorphy of squamates (Estes et al., 1988). The ontogeny of skeletal fusions of *Sphaerodactylus* is similar to *Coleonyx* and *Gonatodes*, where fusion is complete before sexual maturity (Maisano, 2002). The developmental origin of the paroccipital process (pop, Figs. 6B–D and 7I) in adult lepidosaurs has been attributed to the opisthotic exclusively (Jollie, 1960). In *S. roosevelti*, the paroccipital process limits the quadrate posterodorsally, and the posterior process of squamosal (spp, Fig. 4H) is positioned between them. The *fenestra ovalis* (fov, Figs. 2C and 7I,J) lies below the articulation of quadrate and otooccipital.

The three foramina posterior to the oval occipital recess are not confluent as has been proposed for sphaerodactylines (Grismer, 1988). In all the *Sphaerodactylus* and *Gonatodes* examined, they were clearly separated.

In sphaerodactyls the dentary is large, extending posteriorly beyond to the coronoid. In other geckos (e.g., *Coleonyx*, *Uroplatus*) the dentary is shorter, and the splenial is the one extending back to the coronoid. This observation leads to two possible alternatives that can be resolved with developmental studies: 1) with the loss of the splenial, the dentary increased its size, or 2) the splenial fused to the dentary.

The coronoid process is low in sphaerodactyls (Rivero-Blanco, 1976), something that has been correlated with the miniaturization of the skull in this group (Rieppel, 1984b; Abdala, 1996). Kluge (1995) described a character pertaining to coronoid height for sphaerodactyls, scoring a short coronoid for *Coleodactylus, Pseudogonatodes,* and *Sphaerodactylus* and a tall coronoid for *Gonatodes*, *Lepidoblepharis*. We observed all sphaerodactyls to have low coronoids (i.e., hardly elevated above mandible outline), in which the heights are very similar.

The identity of the bones in the rear portion of the jaw in the Gekkota is unclear. Early works commonly identified the two elements as the surangular and the articular (Kluge, 1962; Häupl, 1980; Rieppel, 1984c; Abdala, 1996). Rivero-Blanco (1976) labeled the articular in his figures, but used angular in his descriptions. He described the angular as a bone formed by the prearticular and the ossified Meckel's cartilage. The angular can be present or lost among gekkotans (Estes et al., 1988); pending a detailed embryological study of these geckos, a decision cannot be made as to whether the angular is fused surely or has simply been lost.

Size and Miniaturization of the Skull

Miniaturization has been reviewed in the context of the lizard skull (Rieppel, 1984b) and more generally among tetrapods (Rieppel, 1996). Several features have been identified as indicators of miniaturization. The most evident feature is the reduced skull diameter; as the absolute size of the skull decreases, the relative size of the neurocranium increases (Rieppel, 1984b) and consequently the dermatocranium and the neurocranium lie at the same level. The post-temporal fossae, which are the spaces at the back of the skull between the supraoccipital (neurocranium) and the parietal (dermatocranium), reduce their size with the reduction of the skull diameter. At skull lengths of 15 mm or less, the post-temporal fossae are closed (Rieppel, 1984b). In miniaturized gekkotans, the posterior part of the skull is limited exclusively by the basioccipital, otooccipital, and supraoccipital with no participation of the postparietal process of the parietal and the squamosal bone. This gives the skull a posterolateral edge that is more rounded in miniaturized sphaerodactylids (Fig. 9E–K) than in large ones (Fig. 9A–D) where this corner of the skull is almost flat. This modification shifts the paroccipital process of the otooccipital, and consequently the quadrate bone and the auditory meatus, to a more anterolateral position. Although these structural changes are not exclusively found in sphaerodactylines; they differentiate them from the remaining Sphaerodactylidae.

The relative size of the otic capsules increases as the skull miniaturizes. This has a remarkable effect on the anatomy of the middle ear, which is expected to be allometrically enlarged in young individuals and small species (Werner et al., 2005).

Three criteria may be used to determinate whether a skull is miniaturized or not: the leveling of the rear part of the skull, skull length, and closure of the post-temporal fossae. All the sphaerodactylines fulfill these criteria, so they have miniaturized skulls. Rieppel (1984b) reported adult skull lengths between 4 and 8 mm for the pygopodids *Pletholax* and *Aprasia repens.* The skull length of

S. roosevelti is slightly greater than that of these miniaturized skulls. Another consequence of the reduction in skull diameter is the decrease in space for the jaw adductor muscles. Among gekkotans this is not very critical, as they lost the upper temporal arch (i.e., the connection between postorbitofrontal and the squamosal). Consequently the supratemporal and the infratemporal fenestrae are combined in a single space for these muscles. In gekkotans the jugal-postorbital connection is also lost, so the posterior margin of the orbit is not surrounded by bone. All these modifications of the gekkotan skull cause an increase in the area of attachment of the jaw adductor muscles and the extensor neck muscles, which in miniaturized gekkotans move forward onto the parietal bone, increasing the area covered by these muscles.

In all sphaerodactylines geckos the frontoparietal suture is located about halfway along the total skull length, so the ratio between the muzzle and the parietal units is almost 1:1. In other genera of the Sphaerodactylidae, such as *Teratoscincus*, *Quedenfeldtia*, *Aristelliger*, and *Pristurus*, this ratio is 2:1. One reason for the proportionately longer muzzle in these forms is the lesser degree of overlap of bones in this unit. Remarkably, *Saurodactylus,* which is the sister group of the New World sphaerodactyls shows the 1:1 ratio, but not as the result of an increment in the overlap among the bones of muzzle unit but by shortening of the nasal bones (Fig. 9E). The skull anatomy is greatly different in similar-sized forms such as *Quedenfeldtia* and *Gonatodes* that exploit different substrates, rocky and sandy environments in the former and leaf litter in the latter; this might be an important factor in shaping the skull.

Some other ways in which miniaturized gekkotans differ from other miniaturized squamates are the proportional increase in eye diameter, the preservation of the mesokinetic joint, and the increase in overlap of bones in the snout. In some miniaturized gekkotans such as sphaerodactyls and pygopodids the premaxilla is much enlarged, approaching and reaching the frontal bone. Although the general shape of the skull in these two forms is very different, it is possible that the same condition was developed in parallel to reinforce the skull during the miniaturization process.

General Remarks

The gekkotan skull is highly kinetic, because of the occurrence of osteological modifications such as freeing of the quadrate from the snout unit, and loss of the supratemporal and postorbital bars. The source of these losses has been explained by constructional constraints (Herrel et al., 2000) or paedomorphosis (Rieppel, 1993).

The miniaturization process is thought to be physiologically constrained by the brain and sense organs (Rieppel, 1984b, 1996); this is evident in their relatively massive neurocrania. An additional feature that we observed in the sphaerodactyls is the increase of overlap of elements in the muzzle unit, where this is more common than in the rest of the skull. These geckos, when compared with larger gekkotans, seem to present a miniaturization pattern where their muzzle unit bones retain ancestral dimensions by increasing the overlap areas; as a consequence, the unit is reinforced via butt-lap joints. This pattern is convergent on the limbless pygopodids, which show similar topographic relationships among the rostral bones. The development of butt-lap joints in the rostrum provides a structural advantage because they maximize the joint area while minimizing the profile. This can be important for miniaturized forms, since this increases the resistance to mechanical stress caused during feeding or burrowing. When cornered either in the soil or inside of plastic bags, *Sphaerodactylus* geckos push their heads powerfully back and forth in a series two or three of quick movements. In one opportunity one of us (JDD) observed a male *S. roosevelti* pushing himself through coarse substrate, confirming that they can use the snout for burrowing as escape strategy. Another aspect of the low profile and slender muzzles of sphaerodactyls appears to be that they facilitate binocular overlap of the visual fields, which is so evident when these lizards are stalking their prey (R. Thomas pers. obs. 1966) and is likewise supported by the position of the temporal foveae (Underwood, 1954).

The higher degree of the overlap of bones in the muzzle unit in the miniaturized sphaerodactyls might also be related to their unique habitat. Many, especially the smallest New World sphaerodactyls, inhabit the mat of leaf litter in Neotropical habitats (Barbour, 1921; Thomas et al., 1998; Vitt et al., 2005). In these microhabitats the substrate structure is very complex, and it might require these animals to use their snout in their locomotion. Both the complex habitat and limited space could be an important factor in shaping of the skull and size reduction which is also true for some gymnophthalmid lizards that occur in sympatry with sphaerodactylids.

The adult terminal ossification of *Sphaerodactylus* geckos is comparable to that of closely related genera (e.g., *Gonatodes*) as well as distantly related ones (e.g., *Coleonyx*) (Maisano, 2000, 2002), based on existing phylogenetic hypothesis (Kluge, 1987; Townsend et al., 2004; Conrad and Norell, 2006; Gamble et al., 2008a; Conrad, 2008). Embryological studies may help to clarify details about the formation of the postorbitofrontal, sphenoid, and the compound bone of the lower jaw.

The study of each skull bone in these forms provides a better understanding of its topographic relationships and will be useful as a source of

characters for future studies on the gekkotan tree of life. The skull of gekkotans is extremely diverse and thus is a good source of characters suitable for cladistic analysis. At present, the few morphological studies that have examined broad-scale intergeneric affinities among some subfamilies are restricted to foot structure (Russell, 1976). New primary homologies exclusive for the sphaerodactyls, such as the D-shaped infraorbital fenestra may be helpful for the identification of their sister taxa.

ACKNOWLEDGMENTS

We thank Susan E. Evans (Department of Anatomy and Developmental Biology, University College London) and Jacques Gauthier (Department of Geology and Geophysics, Yale University) for information and comments on the manuscript. We are especially grateful to Jack Conrad and Tony Gamble for access to relevant manuscripts. We also received comments from Jessie Maisano, Ricardo Montero, Victor Hugo Reynoso, and Yehudah L. Werner, all of whom helped to improve the discussion. Darrel Frost and David Kizirian helpfully provided access to skeletal material in the American Museum of Natural History in New York, as did Maureen Kearney and Alan Resetar of the Field Museum in Chicago and Hussam Zaher, Museu de Zoologia da Universidade de São Paulo. We thank the following persons who provided assistance in various ways: T. Mitchell Aide, Gonzalo Aranibar, Wilmar Bolivar, Ana M. Camacho, Fernando Castro-H, David L. Bruck, Alexandra Herrera, Adriana Jerez, Luis Padilla, Robert J. Pascocello, Eugenio Santiago, and Tristan Stayton. It is an extension of a Masters Thesis project by the senior author at the same institution.

LITERATURE CITED

Abdala V. 1990. Descripción osteologíca de *Homonota horrida* (Sauria Gekkonidae). Acta Zool Lilloana 39:31–38.

Abdala V. 1996. Osteología craneal y relaciones de los geconinos sudamericanos (Reptilia: Gekkonidae). Rev Esp Herp 10:41–54.

Abdala V. 1998. Análisis cladístico del género *Homonota* (Gekkonidae). Rev Esp Herp 12:55–62.

Albino A. 2005. A late quaternary lizard assemblage from the southern Pampean region of Argentina. J Paleontol 25:185–191.

Alifanov VR. 1989. The oldest gecko (Lacertilia, Gekkonidae) from the lower cretaceous of Mongolia. Paleontol Zh 1:124–126 (In Russian).

Alifanov VR. 2000. The fossil record of Cretaceous lizards from Mongolia. In: Benton MJ, Shishkin MA, Unwin DM, Kurochkin EN, editors. The Age of Dinosaurs in Russia and Mongolia. Cambridge: Cambridge University Press. pp 368–389.

Barbour T. 1921. Sphaerodactylus. Mem Mus Comp Zool 47:217–278.

Bauer AM. 1989. Extracraneal endolymphatic sacs in *Eurydactylus* (Reptilia: Gekkonidae), with comments on endolymphatic fuction in lizards. J Herpetol 23:172–175.

Bauer AM. 1990a. Phylogenetic systematics and biogeography of the Carphodactylini (Reptilia: Gekkonidae). Bonn Zool Monogr 30:1–218.

Bauer AM. 1990b. Phylogeny and biogeography of the geckos of southern Africa and the islands of the western Indian Ocean: A preliminary analysis. In: Peters G, Hutterer R, editors. Vertebrates in the Tropics. Bonn: Zologisches Forschungsinstitut und Museum A. Koenig. pp 274–284.

Bauer AM, Russell AP. 1989. Supraorbital ossifications in geckos (Reptilia: Gekkonidae). Can J Zool 67:678–684.

Baur G. 1889. On the morphology of the vertebrate skull. J Morphol 3:467–474.

Bell CJ, Evans SE, Maisano JA. 2003. The skull of the gymnophthalmid lizard *Neusticurus ecpleopus* (Reptilia: Squamata). Zool J Linn Soc 103:283–304.

Bellairs AdA, Kamal AM. 1981. The chondrocranium and the development of the skull in recent reptiles. In: Gans C, editor. Biology of the Reptilia. New York: Academic Press.

Bernstein P. 1999. Morphology of the nasal capsule of Heloderma suspectum with comments on the systematic position of helodermatids (Squamata: Helodermatidae). Acta Zool (Stockholm) 80:219–230.

Bever GS, Bell CJ, Maisano JA. 2005. The ossified braincase and cephalic osteoderms of *Shinisaurus crocodilurus* (Squamata, Shinisauridae). Palaeontol Electron 8:36.

Borsuk-Bialynicka M. 1990. Gobekko cretacicus gen. et. sp. n., a new gekkonid lizard from the Cretaceous of the Gobi Desert. Acta Palaeontol Pol 35:67–76.

Brochu CA. 1995. Heterochrony in the crocodylian scapulocoracoid. J Herpetol 29:464–468.

Brock GT. 1932. Some developmental stages in the skulls of geckoes, *Lygodactylus capensis* and *Pachydactylus maculosa*, and their bearing on certain important problems in lacertilian craniology. S Afr J Sci 29:508.

Bustard HR. 1968. The egg-shell of gekkonid lizards: A taxonomic adjunct. Copeia 1968:162–164.

Caldwell MW. 1999. Description and phylogenetic relationships of a new species of *Coniasaurus Owen*, 1850 (Squamata). J Vert Paleontol 19:438–455.

Camp CL. 1923. Clasification of the lizards. Bull Amer Mus Nat Hist 48:289–307.

Carroll RL. 1988a. Late paleozoic and early mesozoic lepidosauromorphs and their relation to lizard ancestry. In: Estes R, Pregill G, editors. Phylogenetic Relationships of the Lizard Families. Essays Commemorating Charles L Camp. Stanford, California: Stanford University Press. pp 99–118.

Carroll RL. 1988b. Vertebrate Paleontology and Evolution. New York: W. H. Freeman. 698 p.

Carroll RL, editor. 1991. The Origin of Reptiles. New York: Cornell University Press. pp 331–353.

Carroll RL, Baird D. 1972. Carboniferous stem-reptiles of the family Romeriidae. Bull Mus Comp Zool 143:321–363.

Cogger HG. 1964. The comparative osteology and systematic status of the gekkonid genera *Afroedura* Loveridge and *Oedura* Gray. Proc Linn Soc NSW 89:364–372.

Conrad JL. 2004. Skull, mandible, and hyoid of *Shinisaurus crocodilurus* Ahl (Squamata: Anguimorpha). Zool J Linn Soc 141:399–434.

Conrad JL. 2008. Phylogeny and systematics of Squamata (Reptilia) based in morphology. Bull Amer Mus Nat Hist 310:1–183.

Conrad JL, Norell M. 2006. High-resolution X-ray computed tomography of an Early Cretaceous gekkonomorph (Squamata) from Öösh (Övorkhangai; Mongolia). Hist Biol 18:405–431.

de Beer GR. 1937. The Development of the Vertebrate Skull. Oxford: Clarendon Press. 552 p.

de Pinna MC. 1991. Concepts and tests of homology in the cladistic paradigm. Cladistics 7:367–394.

Deep-Scaly-Project. 2007a. *Phelsuma lineata* (On-line), Digital morphology. Available at:http://www.digimorph.org.

Deep-Scaly-Project. 2007b. *Phyllurus cornutus* (On-line), Digital morphology. Available at:http://www.digimorph.org.

Dingerkus G, Uhler LD. 1977. Enzyme clearing of alcian blue stained whole small vertebrates for demostration of cartilage. Stain Technol 52:229–232.
Donnellan SC, Hutchinson MN, Saint KM. 1999. Molecular evidence for the phylogeny of Australian gekkonoid lizards. Biol J Linn Soc 67:97–118.
Edmund AG. 1969. Dentition. In: Gans C, editor. Biology of the Reptilia. New York: Academic Press. pp 117–200.
El-Toubi MR, Kamal AM. 1961. The development of the skull of *Ptyodactylus hasselquistii*. III. The osteocranium of a late embryo. J Morphol 108:193–202.
Estes R. 1983. Sauria Terrestria, Amphisbaenia. Stuttgart, New York: Gustav Fischer Verlag. p 249.
Estes R, de Queiroz K, Gauthier J. 1988. Phylogenetic relationships within Squamata. In: Estes R, Pregill G, editors. Phylogenetic Relationships of the Lizard Families. Essays commemorating Charles L Camp. Stanford, California: Stanford University Press. pp 119–281.
Evans SE. 2003a. At the feet of the dinosaurs: The early history and radiation of lizards. Biol Rev 78:513–551.
Evans SE. 2003b. *Nephrurus levis* (On-line), Digital morphology. Available at:http://www.digimorph.org.
Evans SE, Barbadillo LJ. 1998. An unusual lizard (Reptilia: Squamata) from the early cretaceous of Las Hoyas, Spain. Zool J Linn Soc 124:235–265.
Evans SE, Klembara J. 2005. A choristoderan reptile (Reptilia: Diapsida) from the Lower Miocene of Northwest Bohemia (Czech Republic). J Vert Paleontol 25:171–184.
Evans SE, Wang Y. 2005. Early cretaceous lizard *Dalinghosaurus* from China. Acta Palaeontol Pol 50:725–742.
Evans SE, Raia P, Barbera C. 2004. New lizards and rhynchocephalians from the lower cretaceous of southern Italy. Acta Palaeontol Pol 49:393–408.
Fabián-Beurmann ME, Ibarra-Vieira M, Alves MLM. 1980. Estudo osteológico comparativo do cranio de *Hemidactylus mabouia* (Morreau de Jonnes, 1818) e *Homonota uruguayensis* (Vaz Ferreira & Sierra de Soriano, 1961) (Lacertilia, Gekkonidae). Rev Bras Biol 40:187–202.
Frazzetta TH. 1962. A functional consideration of cranial kinesis in lizards. J Morphol 111:287–319.
Frazzetta TH. 1986. The origin of amphikinesis in lizards. Evol Biol 20:419–461.
Gamble T, Bauer AM, Greenbaum E, Jackman TR. 2008a. Evidence for Gondwanan vicariance in an ancient clade of gecko lizards. J Biogeo 35:88–104.
Gamble T, Bauer AM, Greenbaum E, Jackman TR. 2008b. Out of the blue: a novel, trans-Atlantic clade of geckos (Gekkota, Squamata) Zool Scripta 37:355–366.
Gao K, Norell M. 2000. Taxonomic composition and systematics of Late Cretaceous lizard assemblages from Ukhaa Tolgod and adjacent localities, Mongolian Gobi Desert. Bull Am Mus Nat Hist 249:1–118.
Gardiner BG. 1982. Tetrapod classification. Zool J Linn Soc 74:207–232.
Grant C. 1931. The *Sphaerodactylus* of Porto Rico, Culebra and Mona Islands. J Dep Agric PR 15:199–213.
Gravelle K. 1980. Field observations on the use of the tonge-Jacobson's organ system in two iguanid lizards, *Sceloporus jarrovi* and *Anolis trinitatis*. Copeia 1980:356–359.
Greer AE. 1976. On the ocurrence of stapedial foramen in living non-gekkonid lepidosaurs. Copeia 1976:591–592.
Greer AE. 1990. The Biology and Evolution of Australian Lizards. Sydney: Surrey Beatty & Sons Pty Limited. 264 p.
Grismer LL. 1988. Phylogeny, taxonomy, classification, and biogeography of eublepharid geckos. In: Estes R, Pregill G, editors. Phylogenetic Relationships of the Lizard Families. Essays commemorating Charles L Camp. Stanford, California: Stanford University Press. pp 369–469.
Hadley A. 2006. CombineZ5.3 Program and documentation. Available at:http://www.hadleyweb.pwp.blueyonder.co.uk. (Distributed by author).
Häfferl A. 1921. Das knorpelige Neurocranium des Gecko (*Platydactylus annularis*). Z Anat Entwicklungs 62:433–518.
Hallermann J. 1994. Zur Morphologie der Ethmoidalregion der Iguania (Squamata)—Eine vergleichend-anatomische Untersuchung. Bonn Zool Monogr 35:1–135.
Han D, Zhou K, Bauer AM. 2004. Phylogenetic relationships among gekkotan lizards inferred from C-mos nuclear DNA sequences and a new classification of the Gekkota. Biol J Linn Soc 83:353–368.
Hass CA. 1991. Evolution and biogeography of West Indian *Spaherodactylus* (Sauria: Gekkonidae): A molecular approach. J Zool Lond 225:525–561.
Häupl VM. 1980. Das Schädelskelett einiger Arten der Fam. Gekkonidae. Ann Naturh Mus Wien 83:479–518.
Hecht MK. 1951. Fossil lizards of the West Indian genus *Aristelliger* (Gekkonidae). Am Mus Novit 1538:1–33.
Hedges SB, Garrido OH. 1993. A new species of gecko (*Sphaerodactylus*) from Central Cuba. J Herpetol 27:300–306.
Hedges SB, Thomas R. 2001. At the lower size limit in amniote vertebrates: a new diminutive lizard from the West Indies. Caribb J Sci 37:168–173.
Herrel A, Aerts P, De Vree F. 2000. Cranial kinesis in geckoes: Functional implications. J Exp Biol 203:1415–1423.
Herrel A, de Vree F, Delheusy V, Gans C. 1999. Cranial kinesis in gekkonid lizards. J Exp Biol 202:3687–3698.
Hoffstetter R. 1962. Revue des recentes acquisitions concernant l'historie et la systematique des squamates. Problemes actuels de paleontologie (evolution des vertebres), Centre National de la recherche Scientifique 281–324.
Hoffstetter R. 1964. Les Sauria du Jurassique supérier et spécialement les Gekkota de Baviére et de Mandchourie. Senckenb Biol 45:281–324.
Jollie MT. 1960. The head skeleton of the lizard. Acta Zool (Stockholm) 41:1–54.
Kamal AM. 1961. The common characters of the geckonid chondrocranium. Anat Anz 109:109–113.
King W. 1962. Systematics of lesser antillean lizards of the genus *Sphaerodactylus*. Bull Florida State Mus Biol Sci 7:1–52.
Kluge AG. 1962. Comparative osteology of the eublepharid genus *Coleonyx* Gray. J Morphol 110:299–332.
Kluge AG. 1967. Higher taxonomic categories of gekkonid lizards and their evolution. Bull Am Mus Nat Hist 135:1–60.
Kluge AG. 1976. Phylogenetic relationships in the lizard family Pygopodidae: An evaluation of theory, methods and data. Misc Publ Mus Zool Univ Mich 152:1–72.
Kluge AG. 1987. Cladistic relationship in the Gekkonoidea (Squamata, Sauria). Misc Publ Mus Zool Univ Mich 173:IV + 54.
Kluge AG. 1995. Cladistic relationships of sphaerodactyl lizards. Am Mus Novit 3139:1–23.
Kluge AG. 2001. Gekkotan lizard taxonomy. Hamadryad 26:1–209.
Kluge AG, Nussbaum RA. 1995. A review of African-Madagascan Gekkonid lizard phylogeny and biogeography (Squamata). Misc Publ Mus Zool Univ Mich 183:20.
Lee MSY. 1998. Convergent evolution and character correlation in burrowing reptiles: Towards a resolution of squamate relationships. Biol J Linn Soc 65:369–453.
Liang Y-S, Wang C-S. 1973. Comparative study of osteology on the house geckos, *Hemidactylus bowringii* (Gray) and *Hemidactylus frenatus* Duméril & Bribon from Taiwan. Fu Jen Stud Nat Sci 7:63–123.
MacLean WP. 1985. Water-loss rates of *Sphaerodactylus parthenopion* (Reptilia: Gekkonidae), the smallest amniote vertebrate. Comp Biochem Physiol A 82:759–761.
Mahendra BC. 1949. The skull of the Indian house-gecko. *Hemidactylus flaviviridis* Rüppell. Proc Zool Soc Bengal 2:29–42.
Maisano JA. 2000. Postnatal skeletal development in squamates: Its relationship to life history and potential phylogenetic informativeness. PhD. Thesis, Yale University, New Haven, CT. p 730.
Maisano JA. 2001. A survey of state of ossification in neonatal squamates. Herpetol Monogr 15:135–157.
Maisano JA. 2002. Terminal fusions of skeletal elements as indicators of maturity in squamates. J Vert Paleontol 22:268–275.
Maisano JA. 2003a. *Coleonyx variegatus* (On-line), Digital morphology. Available at:http://www.digimorph.org.

Maisano JA. 2003b. *Hemitheconyx caudicinctus* (On-line), Digital Morphology. Available at:http://www.digimorph.org.

Mangione S, Montero R. 2001. The endolymphatic sacs in embryos of *Amphisbaena darwini*. J Herpertol 35:524–529.

McDowell SBJ, Bogert CM. 1954. The systematic position of *Lanthanotus* and the affinities of the anguinomorphan lizards. Bull Am Mus Nat Hist 105:1–42.

Montero R, Moro SA, Abdala V. 2002. Cranial anatomy of *Euspondylus acutirostris* (Squamata: Gymnophthalmidae) and its placement in a modern phylogenetic hypothesis. Russ J Herpetol 9:215–228.

Montero R, Abdala V, Moro S, Gallardo G. 2004. Atlas de *Tupinambis rufescens* (Squamata: Teiidae). Anatomía externa, osteología y bibliografía. Cuad Herpetol 18:17–32.

Moody S. 1983. Endolymphatic dacs in lizards: Phylogenetic and functional considerations. SSAR/HL Annual Meeting, Salt Lake City, Utah.

Noble GK. 1921. The bony structure and phyletic relations of *Sphaerodactylus* and allied lacertilian genera, with the description of a new genus. Am Mus Nov 4:1–16.

Oliver PM, Hutchinson MN, Cooper SJB. 2007. Phylogenetic relationships in the lizard genus *Diplodactylus* Gray and resurrection of *Lucasium Wermuth (Gekkota. Diplodactylidae)*. Aust J Zool 55:197–210.

Ota H, Honda M, Kobayashi M, Sengoku S. 1999. Phylogenetic relationships of eublepharid geckos (Reptilia: Squamata): A molecular approach. Zool Sci 16:659–666.

Poe S, Wiens JJ. 2000. Character selection and the methodology of morphological phylogenetics. In: Wiens JJ, editor. Phylogenetic Analysis of Morphological Data. Washington: Smithsonian Institution Press. pp 20–36.

Pratt CW. 1948. The morphology of the ethmoidal region of *Sphenodon* and lizards. Proc Zool Soc Lond 118:171–201.

Pregill GK. 1981. Late Pleistocene herpetofaunas from Puerto Rico. Misc Publ Univ Kansas Mus Nat Hist 71:1–72.

Regalado R. 2006. Reproduction and growth of seven species of dwarf geckos, *Sphaerodactylus* (Gekkonidae), in captivity. Herpetol Rev 37:13–20.

Rehorek SJ, Firth BT, Hutchinson MN. 2000. Can an orbital gland function in the vomeronasal sense? A study of the pygopodid Harderian gland. Can J Zool 78:648–654.

Rieppel O. 1984a. The cranial morphology of the fossorial lizard genus *Dibamus* with a consideration of its phylogenetic relationships. J Zool Lond 204:289–327.

Rieppel O. 1984b. Miniaturization of the lizard skull: Its functional and evolutionary implications. In: Ferguson MWJ, editor. The Structure, Development and Evolution of Reptiles. London: The Zoological Society of London, Academic Press. pp 503–520.

Rieppel O. 1984c. The structure of the skull and jaw adductor musculature of the Gekkota, with comments on the phylogenetic relationships of the Xantusiidae (Reptilia: Lacertilia). Zool J Linn Soc 82:291–318.

Rieppel O. 1993. Patterns of diversity in the reptilian skull. In: Hanken J, Hall BK, editors. The Skull. Chicago: The University of Chicago Press. pp 344–390.

Rieppel O. 1994. The Lepidosauromorpha: an overview with special emphasis on the Squamata. In: Fraser NC, Sues H-D, editors. In the Shadow of the Dinosaurs: Early Mesozoic Tetrapods. New York: Cambridge University Press. pp 23–37.

Rieppel O. 1996. Miniaturization in tetrapods: Consequences for skull morphology. Symposia of the Zoological Society of London number 69: The Zoological Society of London.

Rivero-Blanco CV. 1976. Osteology of the lizard *Gonatodes humeralis* (Guichenot) and other representative species of the genus. MS Thesis, Texas A&M University, TX.

Rivero-Blanco CV. 1979. The neotropical lizard genus *Gonatodes* Fitzinger (Sauria: Sphaerodactylinae). Ph.D. Thesis, Texas A&M University, TX.233 p.

Rohlf FJ. 2006. tpsDIG2. Version 2.05. Available at: http://life.bio.sunysb.edu/morph/.

Röll B, Henkel FW. 2002. Are pygopods just legless geckos? Evidence from retinal structures. Salamandra 38:73–84.

Romer AS. 1970. The Vertebrate Body. London: W. B. Saunders Company. 601 p.

Russell AP. 1976. Some comments concerning interrelationships amongst gekkonine geckos. In: Bellairs AdA, Cox CB, editors. Morphology and Biology of Reptiles, Linnean Society Symposium Series Number 3. London: Academic Press. pp. 217–244.

Schwartz A, Henderson RW. 1991. Amphibians and Reptiles of the West Indies. Descriptions, Distributions and Natural History. Florida: University of Florida Press. 720 p.

Schwenk K. 1988. Comparative morphology of the lepidosaur tongue and its relevance to squamate phylogeny. In: Estes R, Pregill G, editors. Phylogenetic Relationships of the Lizards Families. Stanford: Stanford University Press. pp. 569–598.

Schwenk K. 1993. Are geckos olfactory specialists? J Zool Lond 229:289–302.

Siebenrock F. 1893. Das Skelet von *Uroplates fimbriatus* Schneid. Ann Naturhist Mus Wien 8:517–536.

Stephenson NG. 1960. The comparative osteology of Australian geckos and its bearing on their morphological status. J Linn Soc Zool 44:278–299.

Stephenson NG. 1962. The comparative morphology of the head skeleton, girdles and hind limbs in the Pygopodidae. J Linn Soc Zool 44:627–644.

Stephenson NG, Stephenson EM. 1956. The osteology of the New Zealand geckos and its bearing in their morphological status. Trans R Soc NZ 84:341–358.

Sumida SS, Murphy RW. 1987. Form and function of the tooth crown structure in gekkonid lizards (Reptilia, Squamata, Gekkonidae). Can J Zool 65:2886–2892.

Thomas R. 1965. A new gecko from the Virgin Islands. Q J Fla Acad Sci 28:117–122.

Thomas R, Schwartz A. 1966. *Sphaerodactylus* (Gekkonidae) in the greater Puerto Rico region. Bull Florida State Mus Biol Sci 10:193–260.

Thomas R, Hedges SB, Garrido O. 1998. A new gecko (*Sphaerodactylus*) from the Sierra Maestra of Cuba. J Herpertol 32:66–69.

Torres-Carvajal O. 2003. Cranial osteology of the andean lizard *Stenocercus guentheri* (Squamata: Tropiduridae) and its postembryonic development. J Morphol 255:94–113.

Townsend TM, Larson A, Louis E, Macey JR. 2004. Molecular phylogenetics of Squamata: The position of snakes, amphisbaenians, and dibamids, and the root of the squamate tree. Syst Biol 53:735–757.

Underwood G. 1954. On the classification and evolution of geckos. Proc Zool Soc Lond 124:469–492.

Underwood G. 1957. On lizards of the family Pygopodidae. A contribution to the morphology and phylogeny of the Squamata. J Morphol 100:207–268.

Vitt LJ, Sartorius SS, Avila-Pires TCS, Zani PA, Espósito MC. 2005. Small in a big world: Ecology of leaf-litter geckos in New World tropical forest. Herpetol Monogr 19:137–152.

Wagner GP. 2001. Characters, units and natural kinds: An introduction. In: Wagner GP, editor. The Character Concept in Evolutionary Biology. New York: University of Chicago Press. pp 1–11.

Wassersug R. 1976. A procedure for differential staining of cartilage and bone in formalin fixed vertebrates. Stain Technol 51:131–134.

Webb M. 1951. The cranial anatomy of the South African geckoes *Palmatogecko rangei* (Andersson) and *Oedura karroica* (Hewitt). Ann U Stellenbosch 27A:131–165.

Wellborn V. 1933. Vergleichende osteologishe Untersuchungen an Geckoniden, Eublephariden und Uroplatiden. Sber Ges Naturf Freunde Berlin 1933:126–199.

Werner YL, Safford SD, Seifan M, Saunders JC. 2005. Effects of age and size in the ears of gekkonomorph lizards: Middle-ear morphology with evolutionary implications. Anat Rec A 238:212–223.

Wever EG. 1973. Closure muscles of the external auditory meatus in Gekkonidae. J Herpetol 7:323–329.

Wheeler WC. 2005. Alignment, dynamic homology and optimization. In: Albert VA, editor. Parsimony, Phylogeny, and Genomics. New York: Oxford University Press. pp 71–80.

APPENDIX

Previously published descriptions of gekkotan and fossil gekkonomorph skulls

GEKKONOMORPHA (*Incertae sedis*)—*Gobekko cretacicus* (Borsuk-Bialynicka, 1990), *Hoburogekko sukhanovi* (Alifanov, 1989, 2000); AMNH FR 21444 (Conrad and Norell, 2006).

EUBLEPHARIDAE—*Aeluroscalabotes felinus* (Grismer, 1988), *Coleonyx variegatus* (McDowell and Bogert, 1954; Kluge, 1962; Maisano, 2003a), *Hemitheconyx caudicinctus* (Wellborn, 1933; Rieppel, 1984c; Maisano, 2003b).

PYGOPODIDAE—*Aprasia pulchella* (Stephenson, 1962), *Aprasia repens* (McDowell and Bogert, 1954; Rieppel, 1984b), *Delma fraseri* (McDowell and Bogert, 1954; Stephenson, 1962), *Lialis burtonis* (McDowell and Bogert, 1954; Stephenson, 1962), *Lialis jicari* (Rieppel, 1984c), *Pletholax gracilis* (Stephenson, 1962; Rieppel, 1984b), *Pygopus lepidopodus* (McDowell and Bogert, 1954; Stephenson, 1962; Rieppel, 1984c; Greer, 1990), *Pygopus nigriceps* (McDowell and Bogert, 1954).

CARPHODACTYLIDAE—*Carphodactylus laevis* (Greer, 1990), *Nephrurus asper* (Stephenson, 1960), *Nephrurus deleani* (Bauer, 1990a), *Nephrurus levis* (Stephenson, 1960; Evans, 2003b), *Saltuarius cornutus* (Stephenson, 1960; Deep-Scaly-Project, 2007b).

DIPLODACTYLIDAE—*Diplodactylus vittatus*, *Lucasium damaeum* (Oliver et al., 2007), *Hoplodactylus duvaucelii*, *Naultilus elegans* (Stephenson and Stephenson, 1956), *Oedura monilis* (Cogger, 1964).

GEKKONIDAE—*Afroedura transvaalica platyceps* (Cogger, 1964), *Rhacodactylus cilliatus* (Bauer, 1990a), *Afroedura karroica* (Webb, 1951), *Chondrodactylus bibronii* (Rieppel, 1984c), *Ebenavia inunguis* (Wellborn, 1933), *Gehyra mutilata, Gehyra oceanica* (Wellborn, 1933), *Gekko gecko* (Häfferl, 1921; Wellborn, 1933), *Gekko japonicus*, *Gekko vittatus* (Wellborn, 1933), *Hemidactylus bowringii* (Liang and Wang, 1973), *Hemidactylus flaviviridis* (Mahendra, 1949), *Hemidactylus frenatus* (Liang and Wang, 1973), *Hemidactylus mabouia* (Wellborn, 1933; Fabián-Beurmann et al., 1980), *Homonota horrida** (Abdala, 1990), *Homonota uruguayensis** (Fabián-Beurmann et al., 1980), *Lepidodactylus lugubris* (Wellborn, 1933), *Lygodactylus capensis* (Brock, 1932), *Lygodactylus picturatus* (Wellborn, 1933), *Pachydactylus maculatus* (Brock, 1932; Häupl, 1980), *Pachydactylus rangei* (Webb, 1951), *Phelsuma lineata* (Deep-Scaly-Project, 2007a), *Phyllopezus pollicaris** (Abdala, 1996), *Ptenopus garrulus* (Wellborn, 1933; Häupl, 1980), *Ptychozoon kuhli* (Wellborn, 1933), *Ptyodactylus hasselquistii* (Wellborn, 1933; Häupl, 1980), *Rhoptropus afer*, *Stenodactylus stenodactylus*, *Tarentola delalandi* (Wellborn, 1933), *Tarentola mauritanica** (Wellborn, 1933; Rieppel, 1984b), *Uroplatus fimbriatus* (Siebenrock, 1893; Wellborn, 1933; Häupl, 1980).

SPHAERODACTYLIDAE—*Aristelliger lar* (Hecht, 1951; McDowell and Bogert, 1954), *Gonatodes albogularis* (Rivero-Blanco, 1976), *Gonatodes antillensis* (Rivero-Blanco, 1976), *Gonatodes atricucullaris*, *Gonatodes concinnatus*, *Gonatodes hasemani* (Rivero-Blanco, 1976), *Gonatodes humeralis* (Wellborn, 1933; Rivero-Blanco, 1976), *Gonatodes seigliei*, *Gonatodes taniae*, *Gonatodes vittatus* (Rivero-Blanco, 1976), *Pristurus carteri* (Häupl, 1980), *Saurodactylus mauritanicus* (Wellborn, 1933), *Sphaerodactylus macrolepis* (Noble, 1921), *Sphaerodactylus molei* (Rieppel, 1984b).

*Taxa marked with asterisks have been assigned to a seventh gekkotan family, Phyllodactylidae, removed from the Gekkonidae on the basis of a phylogenetic analysis published subsequent to the initial acceptance of this paper (Gamble et al., 2008b).